

RE: A point-to-point response to Reviewer #1's comments

“Detection of atmospheric gaseous amines and amides by a high resolution time-of-flight chemical ionization mass spectrometer with protonated ethanol reagent ions” (acp-2016-484) by Lei Yao, Ming-Yi Wang, Xin-Ke Wang, Yi-Jun Liu, Hang-Fei Chen, Jun Zheng, Wei Nie, Ai-Jun Ding, Fu-Hai Geng, Dong-Fang Wang, Jian-Min Chen, Douglas R. Worsnop, and Lin Wang

We are grateful to the helpful comments from this anonymous referee, and have carefully revised our manuscript accordingly. A point-to-point response to Reviewer #1's comments, which are repeated in italic, is given below.

Reviewer #1's comments:

The authors make simultaneous measurements of amines and amides using a recently developed online instrument, the HR-ToF-CIMS. They use ethanol as the reagent ion to optimize the detection of nitrogen-containing molecules. The instrument characteristics within the laboratory context are thorough and well presented, and include calibrations, relative humidity dependence measurements and organic effect on the measured concentrations.

The calibrated HR-ToF-CIMS was then employed to make ambient air measurements of a wide range of amines and amides at an urban site in Shanghai. The ambient measurements answer some questions about sources, sinks and transport of amines and amides and has the potential to be a useful reference for future work on the fate of organic nitrogen compounds in the atmosphere.

In particular, the manuscript is well presented with clear experimental detail. However, the referencing is generally incomplete and careful attention should be taken to research the literature accurately.

Reply: We are very grateful to the positive viewing of our manuscript by Reviewer #1, and have now revised our manuscript accordingly.

General comments:

- 1. The introduction section describing previous measurements of amines and amides is a little tedious to read. Table 2 serves as a good summary and a clear reference and so perhaps the introduction could solely focus on identified trends in season, location, etc. It would also be important to keep referencing Table 2 in the discussion section. Finally, there could be value in making two tables, one for amines and one for amides. This arrangement would also highlight how few amide measurements exist. Also, see comment below for missing references.*

Reply: We have revised our manuscript accordingly. Table 2 has now been divided into two tables, and previous works on amides are shown in Table 3. The main text in the discussion has been

revised accordingly.

2. *The referencing for previous work on amides is incomplete. Amides have been measured and speciated in the context of cigarette smoke and in charbroiling burgers. In addition, they have been identified in PM. See the following references for examples.*

Reply: We have added the related references, although particulate amides are not a focus of this study.

3. *In Table S1, CHNO-H⁺ at m/z 44 is not reported and the authors explain that the proton affinity of HNCO is higher than that of ethanol in their response. Nonetheless, it would be important to mention this simply because of the growing interest in HNCO in our community.*

Reply: Statements on detection of HNCO have been added in the main text, which reads (line 376-379),

“One important atmospheric nitrogen-containing compound, isocyanic acid (HNCO) (Roberts et al., 2011) is not listed in Table S1, because the proton affinity of isocyanic acid is 180.0 kcal mol⁻¹, which is less than that of ethanol (185.6 kcal mol⁻¹). Hence, the ethanol reagent ions are not sensitive to the detection of isocyanic acid.”

4. *2-aminoethanol (m/z 62) is an important industrial compound, especially in carbon capture and storage technologies and is listed in Table S1. Did the concentrations of this compound show high concentrations and/or wind speed/direction dependencies? Perhaps add a short discussion in section 3.2.1.*

Reply: No calibration was performed for 2- aminoethanol, which pre-excludes the determination of its concentration in this study. In addition, no correlation was found between 2-aminoethanol and C₃-amide.

5. *The authors mention the use of the FIGAERO inlet and it is fair that they plan on reporting the particle measurements elsewhere. However, in the context of organic nitrogen it could be important to include a short discussion on how the gas phase and particle phase concentrations of organic nitrogen differ.*

Reply: A pervious study reported that the concentrations of particulate primary amines measured with Fourier transform infrared spectroscopy (FTIR) from micron and submicron particles were 2 orders of magnitude higher than those of gas-phase amines (You et al., 2014). As a conclusion from that specific study, most of amines existed in particles.

We are now working on an optimized quantification method for particulate amines and amides, and other organic nitrogen compounds. It is premature from our dataset to make any statement on how the gas phase and particle phase concentrations of organic nitrogen differ at this stage.

6. *How confident are the authors that their reported concentrations are solely gas phase? What possible contribution could there be from amines and amides in the particle phase?*

Reply: First of all, the FIGAERO inlet has two separate sampling ports: one for gases, and the other for particle collection and subsequent thermal desorption (Lopez-Hilfiker et al., 2014). The temperature of IMR (ion-molecule reactions chamber) was set at 50 °C to minimize the absorption and adsorption of amines and amides on the surface of IMR. Also, our inlet memory tests clearly suggest that the particle analysis (of amines and amides) will not have an impact on the gas sample analysis.

We do not filter out particles in the flow when we analyze gas samples. However, given the pressure in IMR (~100 mbar) and the existence state of amines and amides in aerosols, particulate amines and amides are unlikely to evaporate and react with reagent ions (protonated ethanol ions) to make product ions that can be detected by the mass spectrometer. Hence, the interference for amines and amides from particles were negligible.

7. *Many references and important discussions are included in the conclusion section but would perhaps be more appropriate in the discussion section.*

Reply: We have revised the conclusion section and emphasized on discussions in the discussion section. For example, we moved the following statement from the conclusion section to the discussion section (line 368-372).

“Berndt et al. (2014) reported that pyridine was able to enhance nucleation in H₂SO₄/H₂O system. Also, proton affinities of most of these heterocyclic nitrogen-containing compounds are higher than that of ammonia, hence they potentially have the capacity to neutralize atmospheric acidic species (e.g. H₂SO₄, HNO₃ and organic acids) to contribute to secondary particle formation and growth”.

Also, statements in the conclusion section have been moved into the introduction (line 89-91), “Compared with amines, acetamide has a very weak positive enhancement on the nucleation capability of sulfuric acid (Glasoe et al., 2015).”

Specific comments:

1. *Lines 107-108: Could these authors specify what differences they are referring too? Diurnals? Absolute value? Etc.*

Reply: We meant to state that the absolute concentrations were not significantly different in different urban locations, which is clarified in our revised text

2. *Line 125: I believe that the Borduas et al. and Bunkan et al. references used PTR-MS to measure amides and amines and not CIMS. The authors should double check these references.*

Reply: The principle of PTR-MS is similar to CIMS. Both of them utilize chemical ionization

methodology to charge the analytes. Hence, PTR-MS is considered as a sub-category of CIMS.

3. *Line 170: Please clarify this sentence. “Dominantly protonated” compared to the water clusters?*

Reply: We now state (Line 179-181) that “Amines and amides reacted dominantly with protonated ethanol ions ($(\text{C}_2\text{H}_5\text{OH})_n\cdot\text{H}^+$, $n=1, 2$ and 3), compared to water clusters, with the formation of the protonated amines/amides clustering with up to one molecule of ethanol”.

4. *Line 200: When the authors are referring to total ethanol signal, mean the sum of first three dimers with ethanol correct? (also, this sentence seems a bit out of place.)*

Reply: “Total ethanol signal” refers to the sum of the protonated ethanol monomer, dimer and trimer. The variation in total reagent ions between in laboratory calibration and during field measurements is taken into account when ambient concentrations of amines and amides are calculated. We clarify here (Line 211-214) that “The total ethanol reagent ion signals, i.e., the sum of the protonated ethanol monomer, dimer and trimer, during the laboratory calibration were typically ~ 0.32 MHz, which yields a small correction because of the variation in total reagent ions between in laboratory calibration and during field measurements as stated in section 2.4”.

5. *Lines 296-304: Do the authors have a hypothesis as to why the enhancement is larger with amines than with amides? Perhaps because of differences in proton affinity?*

Reply: We now state (Line 319-324) that “At elevated RH, high concentrations of water vapor result in the production of $(\text{H}_2\text{O})_m\text{H}^+$ ($m=1,2$ and 3) and $\text{C}_2\text{H}_5\text{OH}\cdot\text{H}_2\text{O}\cdot\text{H}^+$ ions (Figure S1) (Nowak et al., 2002). Proton transfer reactions of $(\text{H}_2\text{O})_m\text{H}^+$ ($m=1,2$ and 3) and $\text{C}_2\text{H}_5\text{OH}\cdot\text{H}_2\text{O}\cdot\text{H}^+$ with amines and amides might occur leading to the formation of additional protonated amines and amides. In addition, the proton affinities of amines are generally higher than those of amides. Thus, the relative enhancement was more significant for amines.

6. *Lines 305-312: What is the context of this experiment? Have others observed interferences with organics? Give context and appropriate references.*

Reply: We now state (Line 325-328) that “Since a large number of ambient organics can be detected by this protonated ethanol reagent ion methodology as shown later, laboratory measurements of amines and amides in presence of and in absence of organics formed from photo oxidation of α -pinene and p-xylene, respectively, were carried out to examine the influence of organics on detection of amines and amides”.

7. *Lines 345-346: This is an important finding. Since a majority of nitrogen-containing compounds are oxygenated, it would be interesting to see examples of diurnals and to compare them with the amide diurnals. I would encourage the authors to emphasize this point and discuss further the implications of higher order nitrogen-containing compounds, including in the context of particle formation.*

Reply: This is an excellent suggestion, but determination of nitrogen-containing species with $m/z > 163$ from the ambient mass spectra is beyond the scope of this manuscript.

8. *Line 363: “C5 and C6 amines standards are unavailable” is difficult to believe, especially since the authors build their own permeation tubes for the most part. I would recommend the authors clarify or remove this statement.*

Reply: We now state (Line 396-397) that “Since the sensitivities of C₅- to C₆-amine were not determined, the sensitivity of DEA by HR-ToF-CIMS was adopted to quantify C₅- to C₆-amines”

9. *Line 383: a value of 778 +/- 899 is a little bizarre. How were the errors calculated? Line 385-386: I would recommend moving this sentence to the paragraph discussing these high values in section 3.2.4.*

Reply: The error here represents one standard deviation, which is derived from the significant fluctuation in the C₃-amide concentration as shown in Figure 5.

The sentence regarding the high concentration of C₃-amides has been moved to section 3.2.4.

10. *Lines 393-397: What could be the role of particle phase chemistry on the observed diurnals?*

Reply: According to our preliminary uptake experiments of amides by suspended H₂SO₄ particles and published uptake coefficient of amines by sulfuric acid (Wang et al., 2010), heterogeneous chemistry does not show a major preference between amines and amides. The lower RH in the daytime will generally lead to higher particle acidity, but not in the range of acidity that has been studied (Wang et al., 2010). Hence, the role of heterogeneous chemistry is not discussed here.

In the atmospheric condensed-phase material and cloud droplets, amines (e.g. methylamine) can react with aldehydes (e.g. methyglyoxal and glyoxal) to form oligomers that contribute to secondary organic aerosols (De Haan et al., 2009, 2011; Galloway et al., 2014). However, no data on aldehydes in the condensed-phase material and cloud droplets were available during our ambient campaign. Hence, we decided not to estimate the contribution of particle phase chemistry to the observed diurnals.

11. *Figure 2 – Can the authors estimate the concentrations of pinene and xylene used in these experiments? This information would be useful to include in the experimental section starting on line 210.*

Reply: The estimated concentrations of α -pinene and p-xylene were both ~200ppb. We have added the concentrations of these two compounds in main text.

12. *Figure 4 is an important analysis and can be used to discuss functional group interconversion and trends. I would recommend the authors spend a bit more time analyzing these graphs and discussing them.*

Reply: The high-resolution mass spectrometer allows us to determine the molecular formulas of these nitrogen-containing species and hence their mass defects, but would not permit a direct determination of the functional groups. The focus of this manuscript is detection of amines and amides. Interested readers can refer to the supplementary Table S1 that lists the tentative formula assignments for these nitrogen-containing species

13. *Figure 6 is not convincing. The amines and amides seem to have decreased prior to rain fall. Are RH measurements available? Perhaps a better correlation can be seen with RH instead of rainfall?*

Reply: In figure 6, the concentrations of amines and amides started to decrease right after the sunrise on August 21, 2015 (i.e., before the actual rain fall), which is in fact consist with their typical diurnal cycles. We meant to show in Figure 6 that the concentrations of amines and amides are generally maintaining at a low level on raining days, hinting the role of wet deposition. In addition, no clear correlation between RH and the concentrations of amines and amides were observed.

14. *Line 459: specify what is meant by “slightly better”. Because of detection limits, or choice of reagent ion, or?*

Reply: We now state (Line 494-495) that “...are slightly better than those in previous studies using a similar protonated ethanol-CIMS method”, which clarifies that both sensitivities and detection limits are slightly better. .

15. *Lines 480-481: added references: Barnes et al., Borduas et al., Bunkan et al.*

Reply: We have added these references.

Technical comments:

1. *Line 47: missing the word “the” before the word detection.*

Reply: We have revised our manuscript accordingly.

2. *Lines 53-54: separate the sentences; one thought on the diurnal profile of amines and another on the diurnal profiles of amides.*

Reply: We now state (Line 53-54) that “the diurnal profiles and backward trajectory analysis suggest that in addition to the secondary formation of amides in the atmosphere, industrial emissions could be important sources of amides in urban Shanghai”.

3. *Lines 88, 121: physio-chemical should be written as physico-chemical. I think the authors are referring to physical properties and not to physiology properties.*

Reply: We have revised our manuscript accordingly.

4. *Line 187: delete “referred to that as” Lines 328-329: check syntax of the sentence.*

Reply: Line 187 (now Line 198): “referred to that as” has been removed.

Lines 328-329 (now lines 352-354): we now state that “In addition to the protonated C₁ to C₆-amines and amides, the presence of their clusters with one ethanol molecule is evident, which further confirms the identification of these species”.

5. *Lines 433-436: check syntax of the sentence. Line 487: progress is misspelled.*

Reply: Lines 433-436 (now lines 468-471): we now state “Three-day backward retroplumes (100 m above the ground level) from the Fudan sampling site are shown for air masses with mixing ratios of C₃-amides > 2670 pptv in Figure 8, and for air masses with the C₃-amide concentration range between 1340 pptv and 2650 pptv in Figure S10, respectively.”

Line 487: we revised our manuscript accordingly.

References:

- Almeida, J., Schobesberger, S., Kürten, A., Ortega, I. K., Kupiainen-Määttä, O., Praplan, A. P., Adamov, A., Amorim, A., Bianchi, F., Breitenlechner, M., David, A., Dommen, J., Donahue, N. M., Downard, A., Dunne, E., Duplissy, J., Ehrhart, S., Flagan, R. C., Franchin, A., Guida, R., Hakala, J., Hansel, A., Heinritzi, M., Henschel, H., Jokinen, T., Junninen, H., Kajos, M., Kangasluoma, J., Keskinen, H., Kupe, A., Kurtén, T., Kvashin, A. N., Laaksonen, A., Lehtipalo, K., Leiminger, M., Leppä, J., Loukonen, V., Makhmutov, V., Mathot, S., McGrath, M. J., Nieminen, T., Olenius, T., Onnela, A., Petäjä, T., Riccobono, F., Riipinen, I., Rissanen, M., Rondo, L., Ruuskanen, T., Santos, F. D., Sarnela, N., Schallhart, S., Schnitzhofer, R., Seinfeld, J. H., Simon, M., Sipilä, M., Stozhkov, Y., Stratmann, F., Tome, A., Tröstl, J., Tsagkogeorgas, G., Vaattovaara, P., Viisanen, Y., Virtanen, A., Vrtala, A., Wagner, P. E., Weingartner, E., Wex, H., Williamson, C., Wimmer, D., Ye, P., Yli-Juuti, T., Carslaw, K. S., Kulmala, M., Curtius, J., Baltensperger, U., Worsnop, D. R., Vehkamäki, H., and Kirkby, J.: Molecular understanding of sulphuric acid-amine particle nucleation in the atmosphere, *Nature*, 502, 359-363, 10.1038/nature12663, 2013.
- De Haan, D. O.; Tolbert, M. A.; Jimenez, J. L. Atmospheric condensed-phase reactions of glyoxal with methylamine. *Geophys. Res. Lett.* 36, L11819, 2009.
- De Haan, D. O.; Hawkins, L. N.; Kononenko, J. A.; Turley, J. J.; Corrigan, A. L.; Tolbert, M. A.; Jimenez, J. L. Formation of nitrogencontaining oligomers by methylglyoxal and amines in simulated evaporating cloud droplets. *Environ. Sci. Technol.* 45 (3), 984– 991, 2011.
- Galloway, M. M.; Powelson, M. H.; Sedehi, N.; Wood, S. E.; Millage, K. D.; Kononenko, J. A.; Rynaski, A. D.; De Haan, D. O. Secondary Organic Aerosol Formation during Evaporation of Droplets Containing Atmospheric Aldehydes, Amines, and Ammonium Sulfate. *Environ. Sci.*

Technol. 2014, 48 (24), 14417–14425.

- Nowak, J. B.: Chemical ionization mass spectrometry technique for detection of dimethylsulfoxide and ammonia, *J. Geophys. Res. Atmos.*, 107, 10.1029/2001jd001058, 2002.
- Pratt, K. A., Hatch, L.E., Prather, K. A.: Seasonal volatility dependence of ambient particle phase amines, *Environ. Sci. Technol.*, 43, 5276-5281, 10.1021/es803189n, 2009.
- Wang, L., Lal, V., Khalizov, A. F., and Zhang, R. Y.: Heterogeneous Chemistry of Alkylamines with Sulfuric Acid: Implications for Atmospheric Formation of Alkylaminium Sulfates, *Environ. Sci. Technol.*, 44, 2461-2465, 10.1021/es9036868, 2010.
- You, Y., Kanawade, V. P., de Gouw, J. A., Guenther, A. B., Madronich, S., Sierra-Hernández, M. R., Lawler, M., Smith, J. N., Takahama, S., Ruggeri, G., Koss, A., Olson, K., Baumann, K., Weber, R. J., Nenes, A., Guo, H., Edgerton, E. S., Porcelli, L., Brune, W. H., Goldstein, A. H., and Lee, S. H.: Atmospheric amines and ammonia measured with a chemical ionization mass spectrometer (CIMS), *Atmos. Chem. Phys.*, 14, 12181-12194, 10.5194/acp-14-12181-2014, 2014.

RE: A point-to-point response to Reviewer #2's comments

“Detection of atmospheric gaseous amines and amides by a high resolution time-of-flight chemical ionization mass spectrometer with protonated ethanol reagent ions” (acp-2016-484) by Lei Yao, Ming-Yi Wang, Xin-Ke Wang, Yi-Jun, Liu, Hang-Fei Chen, Jun Zheng, Wei Nie, Ai-Jun Ding, Fu-Hai Geng, Dong-Fang Wang, Jian-Min Chen, Douglas R. Worsnop, and Lin Wang

We are grateful to the helpful comments from this anonymous referee, and have carefully revised our manuscript accordingly. A point-to-point response to Reviewer #2's comments, which are repeated in *italic*, is given below.

Reviewer #2's comments:

1. *Lines 93-94: C3 amines include trimethylamine, methyl-ethylamine and propylamine (formally also azetidine and the various methylaziridines, which have a different sum formula)*

Reply: The reported concentrations are the sum of propylamine (PA) and trimethylamine (TMA) (Kieloaho et al. 2013). This statement has been rephrased as “the sum of propylamine (PA) and trimethylamine (TMA)”.

2. *Lines 166-167: It is stated that the amines and amides reacted dominantly with protonated ethanol (through proton transfer reactions). This statement requires some clarification. The authors state in the lines preceeding that most abundant reagent ion is protonated ethanol dimer (illustrated in Fig. S1).*

Reply: Under our CIMS setup, the most abundant reagent ion is the protonated ethanol dimer with the second most dominant ions being protonated ethanol monomer and trimer. The ion-molecule reactions between the analytes and reagent ions leads to the formation of protonated analytes (clustering with up to one molecule of ethanol), which is somehow similar to the conventional proton transfer reactions of hydronium ions. We now clarify (Line 179-181) that “Amines and amides reacted dominantly with protonated ethanol ions $((\text{C}_2\text{H}_5\text{OH})_n \cdot \text{H}^+, n=1, 2 \text{ and } 3)$, compared to water clusters, with the formation of protonated amines/amides clustering with up to one molecule of ethanol.”.

3. *3.1.2 Effects of RH and organics: The influence of RH on the instrument sensitivity is described and illustrated for three simple amines. The observed effect requires some explanation. Have the authors calculated the PTR rate coefficients for the different reagent ions? Does the reagent ion distribution change significantly?*

Reply: As shown in Figure S1, $(\text{H}_2\text{O})_m\text{H}^+$ ($m=1, 2 \text{ and } 3$) and $\text{C}_2\text{H}_5\text{OH} \cdot \text{H}_2\text{O} \cdot \text{H}^+$ are present under elevated RH conditions, both of which are likely more reactive than protonated ethanol dimer (Nowak et al., 2002). Hence, proton transfer reactions of $(\text{H}_2\text{O})_m\text{H}^+$ and $\text{C}_2\text{H}_5\text{OH} \cdot \text{H}_2\text{O} \cdot \text{H}^+$ with

amines and amides may take place leading to the formation of protonated amines and amides. We have now (Line 319-322) state that

“At elevated RH, high concentrations of water resulted in the production of $(\text{H}_2\text{O})_m\text{H}^+$ ($m=1,2$ and 3) and $\text{C}_2\text{H}_5\text{OH}\cdot\text{H}_2\text{O}\cdot\text{H}^+$ ions (Figure S1) (Nowak et al., 2002). Proton transfer reactions of $(\text{H}_2\text{O})_m\text{H}^+$ ($m=1, 2$ and 3) and $\text{C}_2\text{H}_5\text{OH}\cdot\text{H}_2\text{O}\cdot\text{H}^+$ with amines and amides might occur leading to the formation of additional protonated amines and amides.”

We didn't calculate the reaction rates of amines and amides with different reagent ions. Calibration curves with known concentrations of authentic standards were used to derive their ambient concentrations instead, although those curves were obtained at ~0% RH. However, in our ambient measurements, we used high purity nitrogen to dilute the sample flow resulting in an overall RH < 20%, under which RH no significant effect on reagent ions distribution was observed.

4. Line 314: "oxomide" should be "oxamide"

Reply: We have replaced “oxomide” by “oxamide”.

5. Figure 3 requires some additional information/clarification. First, the peak-shape is not discussed. Second, the curve-fitting includes a listing "Isotopes and other compounds". It is not obvious to the reader which "isotopes and other compounds" that are actually included in the analyses. As an example the region around m/z 60 must clearly contain a signal from the 13-C isotope of acetone (60.053), but this appears not to be the case.

Reply: Clarification is now provided in the figure legend, the figure caption, and the main text. The exact formulas for “Isotopes and other compounds” have been provided in the figure legend. The new figure caption reads “**Figure 3.** High-resolution single peak fitting (custom shape) for amines and amides. During the peak deconvolution, only peaks whose areas are more than 0.5% of the total will be included in the figure legend.”

Also, we state (Line 348-349) in the main text that “The assignment of molecular formulas for these species is within a mass tolerance of < 10 ppm, and the fitted area ranges from 99% to 101%”.

We observed protonated acetone (m/z 59.0491) (Table S1) but its arbitrary signal was much less than that of protonated C₂-amide. Hence, the 13-C isotope of acetone, whose abundance is 3.3% of acetone, did not stand out in our mass spectra.

Reference:

- Kieloaho, A.-J., Hellén, H., Hakola, H., Manninen, H. E., Nieminen, T., Kulmala, M., and Pihlatie, M.: Gas-phase alkylamines in a boreal Scots pine forest air, *Atmos. Environ.*, 80, 369-377, 10.1016/j.atmosenv.2013.08.019, 2013.
- Nowak, J. B.: Chemical ionization mass spectrometry technique for detection of dimethylsulfoxide and ammonia, *J. Geophys. Res. Atmos.*, 107, 10.1029/2001jd001058, 2002.

RE: A point-to-point response to Reviewer #3's comments

“Detection of atmospheric gaseous amines and amides by a high resolution time-of-flight chemical ionization mass spectrometer with protonated ethanol reagent ions” (acp-2016-484) by Lei Yao, Ming-Yi Wang, Xin-Ke Wang, Yi-Jun, Liu, Hang-Fei Chen, Jun Zheng, Wei Nie, Ai-Jun Ding, Fu-Hai Geng, Dong-Fang Wang, Jian-Min Chen, Douglas R. Worsnop, and Lin Wang

We are grateful to the helpful comments from this anonymous referee, and have carefully revised our manuscript accordingly. A point-to-point response to Reviewer #3's comments, which are repeated in italic, is given below.

Reviewer #3's comments:

The manuscript presents a method for the quantitative measurement of various amines and amides in the ppt range by Chemical Ionization using a High - Resolution Time - of - Flight mass spectrometer with protonated ethanol reagent ions. Calibrations are presented and the influence of humidity is characterized in the laboratory. Several weeks of ambient measurements in Shanghai are presented. 85 nitrogen - containing species with $m/z < 163$ Th are identified in the ambient air including numerous amines and amides. Amines reach mixing ratios up to more than 100 pptv. Amides reach maximum mixing ratios of several ppbv. Diurnal variations of specific amines and amides are studied.

The paper is well written, concise and well structured. Measurements are made with ethanol as reagent ions, a reagent ion that had not been tested in detail before. Atmospheric measurements of amides with CIMS have not been presented before. The paper is suitable for publication in ACP. Some minor comments should be taken into account.

Reply: We are very grateful to the positive viewing of our manuscript by Reviewer #3, and have now revised our manuscript accordingly.

Minor comments:

1. l. 86: *some important earlier references are missing: Murphy et al., ACP, 7, 2313–2337, 2007; Kurten et al., ACP, 8, 4095–4103, 2008; Berndt et al., ACP, 10, 7101–7116, 2010.*

Reply: These three references have been added.

2. l. 88: *also Bzdek et al., ACP, 10, 3495–3503, 2010 and Kupianinen et al., ACP, 12, 3591–3599, 2012, should be cited.*

Reply: These two references have been added.

3. l. 103 - 105: *compare also with the much lower amine concentrations measured with CIMS in Hyytiälä as presented by Sipilä et al., AMT, 8, 4001–4011, 2015.*

Reply: Inter-comparison with results from Sipilä et al. (2015) is added. We now state (Line 114-117) that “Additionally, at the same site, DMA concentration was measured to be less than 150 ppqv (parts per quadrillion by volume) in May-June 2013 by an atmospheric pressure CIMS based on bisulfate-cluster method for DMA detection (Sipilä et al. 2015).”

4. l. 122 - 123: *Also Sipilä et al. 2015, and Simon et al., AMT, 9, 2135 - 2145, 2016, should be cited.*

Reply: These two references have been cited.

5. l. 139 - 140. *Avoid exact repetition of sentences from the abstract.*

Reply: We have revised our manuscript accordingly.

6. l. 366 - 367: *compare also with the results of Sipilä et al., AMT, 2015.*

Reply: We have added the inter-comparison in discussion section 3.2.2 (line 407-411). We have now state that

“The concentrations of amines in Shanghai are generally smaller than those in Hyytiälä, Finland (Hellén et al., 2014; Kieloaho et al., 2013; Sellegri et al., 2005) except for one study that, as stated by the authors, should be treated with caution (Sipilä et al. 2015), potentially hinting that sources for amines existed in the forest region of Hyytiälä, Finland.”

7. *Table 2: include also Sipilä et al., AMT, 8, 4001–4011, 2015, and Kürten et al., ACPD, doi:10.5194/acp - 2016 - 294, 2016 in the inter - comparison.*

Reply: These two references have been added. We have now state that (line 407-413)

“The concentrations of amines in Shanghai are generally smaller than those in Hyytiälä, Finland (Hellén et al., 2014; Kieloaho et al., 2013; Sellegri et al., 2005) except for one study that, as stated by the authors, should be treated with caution (Sipilä et al. 2015), potentially hinting that sources for amines existed in the forest region of Hyytiälä, Finland. Our C₁- and C₂-amines are generally more abundant than those in agricultural, coastal, continental, suburban, and urban areas (Freshour et al., 2014; Hanson et al., 2011; Kieloaho et al., 2013; Kürten et al., 2016; Sellegri et al., 2005; You et al., 2014).”

8. *Figure 3, upper right hand panel: some discussion of the “isotopes and other compounds” peaks needs to be given. Some more discussion of the uncertainties of the peak separation is necessary. Please discuss why the main peak needs to be separated into the two peaks as indicated. How large are the uncertainties in mass and signal intensity for the “isotopes and other compounds” peak?*

Reply: Clarification is now provided in the figure legend and the figure caption. The exact formulas for “Isotopes and other compounds” have been provided in the figure legend. The new

figure caption reads “**Figure 3.** High-resolution single peak fitting (custom shape) for amines and amides. During the peak deconvolution, only peaks whose areas are more than 0.5% of the total will be included in the figure legend.”

Also, we state (Line 348-349) in the main text that “The assignment of molecular formulas for these species is within a mass tolerance of < 10 ppm, and the fitted area ranges from 99% to 101%”.

Technical corrections:

1. l. 5: *omit comma between Yi - Jun and Liu*

Reply: We have revised our manuscript accordingly.

2. l. 158: *...was THE protonated ethanol...*

Reply: We have revised our manuscript accordingly.

3. l. 159: *... with the SECOND MOST dominant ions being THE protonated ethanol monomer...*

Reply: We have revised our manuscript accordingly.

4. l. 160: *... and THE protonated ethanol trimer*

Reply: We have revised our manuscript accordingly.

5. l. 163: *... the ratios of THE oxygen...*

Reply: We have revised our manuscript accordingly.

6. l. 168: *(...NR₃, with R BEING EITHER A HYDROGEN ATOM or an alkyl group)*

Reply: We have revised our manuscript accordingly.

7. l. 169: *(... WITH R` BEING EITHER A HYDROGEN or ...)*

Reply: We have revised our manuscript accordingly.

8. l. 169 - 170: *... can be REPRESENTED BY THE FOLLOWING REACTIONS (Yue...*

Reply: We have revised our manuscript accordingly.

9. l. 209: *mixed WITH the amine/amide...*

Reply: We have revised our manuscript accordingly.

10. l. 359: ...*each DATA point*...

Reply: We have revised our manuscript accordingly.

11. l. 421: *A Lagrangian*...

Reply: We have revised our manuscript accordingly.

12. l. 425: ... *are SHOWN for air masses*

Reply: We have revised our manuscript accordingly.

**Detection of atmospheric gaseous amines and amides by a high resolution
time-of-flight chemical ionization mass spectrometer with protonated
ethanol reagent ions**

Lei Yao¹, Ming-Yi Wang^{1,2†}, Xin-Ke Wang¹, Yi-Jun Liu^{1,23}, Hang-Fei Chen¹, Jun ~~Zheng~~³~~Zheng~~⁴, Wei
~~Nie~~⁴~~Nie~~^{5,56}, Ai-Jun ~~Ding~~⁴~~Ding~~^{5,56}, Fu-Hai ~~Geng~~⁶~~Geng~~⁷, Dong-Fang ~~Wang~~⁷~~Wang~~⁸, Jian-Min Chen¹,
Douglas R. ~~Worsnop~~⁸~~Worsnop~~⁹, Lin Wang^{1,56*}

¹ Shanghai Key Laboratory of Atmospheric Particle Pollution and Prevention (LAP³), Department of
Environmental Science & Engineering, Fudan University, Shanghai 200433, China

² now at Center for Atmospheric Particle Studies, Carnegie Mellon University, Pittsburgh, PA 15213,
USA

²⁻³ now at Pratt School of Engineering, Duke University, Durham, NC 27705, USA

³⁻⁴ Jiangsu Key Laboratory of Atmospheric Environment Monitoring and Pollution Control, Nanjing
University of Information Science & Technology, Nanjing 210044, China

⁴⁻⁵ Joint International Research Laboratory of Atmospheric and Earth System Sciences, School of
Atmospheric Science, Nanjing University, 210023, Nanjing, China

⁵⁻⁶ Collaborative Innovation Center of Climate Change, Nanjing, Jiangsu Province, China

⁶⁻⁷ Shanghai Meteorology Bureau, Shanghai 200135, China

⁷⁻⁸ Shanghai Environmental Monitoring Center, Shanghai 200030, China

⁸⁻⁹ Aerodyne Research, Billerica, MA 01821, USA

* Corresponding Author: L.W., email, lin_wang@fudan.edu.cn; phone, +86-21-65643568; fax,
+86-21-65642080.

Abstract

Amines and amides are important atmospheric organic-nitrogen compounds but high time resolution, highly sensitive, and simultaneous ambient measurements of these species are rather sparse. Here, we present the development of a high resolution time-of-flight chemical ionization mass spectrometer (HR-ToF-CIMS) method utilizing protonated ethanol as reagent ions to simultaneously detect atmospheric gaseous amines (C_1 to C_6) and amides (C_1 to C_6). This method possesses sensitivities of 5.6-19.4 Hz pptv⁻¹ for amines and 3.8-38.0 Hz pptv⁻¹ for amides under total reagent ion signals of ~0.32 MHz, and detection limits of 0.10-0.50 pptv for amines and 0.29-1.95 pptv for amides at 3 σ of the background signal for a 1-min integration time, respectively. Controlled characterization in the laboratory indicates that relative humidity has significant influences on the detection of amines and amides, whereas the presence of organics has no obvious effects. Ambient measurements of amines and amides utilizing this method were conducted from 25 July 2015 to 25 August 2015 in urban Shanghai, China. While the concentrations of amines ranged from a few pptv to hundreds of pptv, concentrations of amides varied from tens of pptv to a few ppbv. Among the C_1 - to C_6 -amines, the C_2 -amines were the dominant species with concentrations up to 130 pptv. For amides, the C_3 -amides (up to 8.7 ppb) were the most abundant species. The diurnal and backward trajectory analysis profiles of amines and amides suggest that in addition to the secondary formation of amides in the atmosphere, industrial emissions could be important sources of amides in urban Shanghai. During the campaign, photo-oxidation of amines and amides might be a main loss pathway for them in day time, and wet deposition was also an important sink.

1 Introduction

Amines and amides are nitrogen-containing organic compounds widely observed in the atmosphere ([Cape et al., 2011](#); [Cheng et al., 2006](#); Ge et al., 2011; [Laskin et al., 2009](#); [Rogge et al., 1991](#)). They are emitted from a variety of natural and anthropogenic sources including agriculture, biomass burning, animal husbandry, cooking, [smoking](#), synthetic leather, carbon capture, and other industrial processes (Finlayson-Pitts and Pitts, 2000; Ge et al., 2011; Kim et al., 2004; Kuhn et al., 2011; Nielsen et al., 2012; [Schmeltz et al., 1977](#); Zhu et al., 2013). In addition to the primary sources, amides can be formed from the degradation processes of amines (Nielsen et al., 2012) and atmospheric accretion reactions of organic acids with amines or ammonia (Barsanti and Pankow, 2006).

Once in the atmosphere, amines and amides can react with atmospheric oxidants (*e.g.*, OH and NO₃ radicals, Cl atoms, and O₃), and lead to gaseous degradation products and formation of secondary organic aerosols (Barnes et al., 2010; Bunkan et al., 2016; El Dib and Chakir, 2007; Lee and Wexler, 2013; Malloy et al., 2009; Murphy et al., 2007; Nielsen et al., 2012). In addition, the basic nature of amines certainly justifies their participation in atmospheric new particle formation and growth events (Almeida et al., 2013; [Berndt et al., 2010](#); Erupe et al., 2011; Glasoe et al., 2015; [Kurtén et al., 2008](#); [Murphy et al., 2007](#); Smith et al., 2010; Yu et al., 2012; Zhang et al., 2012). [Compared with amines, acetamide has a very weak positive enhancement on the nucleation capability of sulfuric acid \(Glasoe et al., 2015\)](#). Heterogeneous uptake of amines by acidic aerosols and displacement reactions of ammonium ions by amines can significantly alter the physico-chemical properties of aerosol particles ([Bzdek et al., 2010](#); [Kupiainen et al., 2012](#); Qiu et al., 2011; Wang et al., 2010a; Wang et al., 2010b).

Atmospheric [gaseous](#) amines have been measured in different surroundings. Kieloaho et al. (2013) used offline acid-impregnated fiberglass filter collection together with analysis by high performance liquid chromatography electrospray ionization ion trap mass spectrometer, and reported that the highest concentrations of C₂-amines (ethylamine (EA) + dimethylamine (DMA)) and [the sum of C₃-amines \(propylamine \(PA\) + and trimethylamine \(TMA\)\)](#) reached 157±20 pptv (parts per trillion by volume) and 102±61 pptv, respectively, in boreal forests, southern Finland. Using a similar detection method, the mean concentrations of C₂-amines (EA+DMA), C₃-amines (PA+TMA), butylamine (BA), diethylamine (DEA) and triethylamine (TMA) were measured to be 23.6 pptv, 8.4

pptv, 0.3 pptv, 0.3 pptv, and 0.1 pptv, respectively, in urban air of Helsinki, Finland (Hellén et al., 2014). Detection of gaseous alkyl amines were conducted in Toronto, Canada using an ambient ion monitor ion chromatography system, and the concentrations of DMA, and TMA+DEA were both less than 2.7 ppt (parts per trillion by volume) (VandenBoer et al. 2011). In addition, Dawson et al. (2014) reported that TMA concentration was up to 6.8 ppbv (parts per billion by volume) in Chino, USA, using an offline ion chromatography analysis method.

Recently, online detection of atmospheric amines using chemical ionization mass spectrometer is becoming the trend. Yu and Lee (2012) utilized a quadrupole chemical ionization mass spectrometer (CIMS) with protonated ethanol and acetone ions as reagent ions to measure C₂-amines (8±3 pptv) and C₃-amines (16±7 pptv) in Kent, Ohio. A similar method detected a few pptv to tens of pptv C₃-amines in Alabama forest (You et al., 2014). Sellegri et al. (2005) reported the mean concentration of TMA and DMA were 59 pptv and 12.2 pptv, respectively, in Hyytiälä forest, with a quadrupole-CIMS with hydronium ions as reagent ions. Additionally, at the same site, DMA concentration was measured to be less than 150 ppqv (parts per quadrillion by volume) in May-June 2013 by an atmospheric pressure CIMS based on bisulfate-cluster method for DMA detection (Sipilä et al. 2015). Measurements of amines in urban areas did not show significant differences in terms of the absolute concentration. The average of total amines (C₁-C₃) was 7.2±7.4 pptv in Nanjing, China, as measured by a high resolution time-of-flight CIMS (HR-ToF-CIMS) with hydronium ions as reagent ions (Zheng et al., 2015). Measurements by an ambient pressure proton transfer mass spectrometer (AmPMS) in urban Atlanta showed that trimethylamine (TMA) (or isomers or amide) was the most abundant amine-species and that the concentration of DMA was ~3 pptv (Hanson et al., 2011).

To the best of our knowledge, gaseous amides were not previously measured in ambient air, except for two studies that briefly described the detection of a few amides near the emission source. Zhu et al. (2013) detected formamide (FA) (C₁-amide) formed from degradation of mono-ethanolamine in emissions from an industrial carbon capture facility, using proton transfer reaction time-of-flight mass spectrometry (PTR-ToF-MS). Furthermore, up to 4350 pptv of dimethylamide was observed near a municipal incinerator, waste collection center and sewage treatment plant (Leach et al., 1999).

Given the important role of amines in atmospheric nucleation and other physico-chemical processes, and the potential involvement of amides in a number of atmospheric processes, it is

necessary to develop high time resolution and highly sensitive detection techniques for measurements of ambient amines and amides. Previous studies have proven CIMS to be a powerful instrument to detect gaseous amines and amides in laboratory studies and field campaigns (Borduas et al., 2015; Bunkan et al., 2016; Hanson et al., 2011; Sellegri et al., 2005; [Simon et al. 2016](#); [Sipilä et al. 2015](#); Yu and Lee, 2012; You et al., 2014; Zheng et al., 2015). However, the detection method for ambient amides with much lower concentrations than those in laboratory studies is still lacking. The popular usage of hydronium ions as reagent ions (*e.g.* PTR-MS and AmPMS) potentially leads to the relative humidity (RH) dependence of the background and ambient amine signals, adding uncertainties to measurement results (Hanson et al., 2011; Zheng et al., 2015; Zhu et al., 2013). In addition, constrained by the mass resolution of the quadrupole-detector mass spectrometer, it is difficult to distinguish protonated amines and amides with an identical unit mass, which pre-excludes the possibility of simultaneous measurements of amines and amides. For example, the m/z (mass to charge ratio) value of protonated trimethylamine ($\text{C}_3\text{H}_9\text{N}\cdot\text{H}^+$, m/z 60.0808) and that of protonated acetamide ($\text{C}_2\text{H}_5\text{NO}\cdot\text{H}^+$, m/z 60.0444) are very close.

In the present study, a HR-ToF-CIMS method utilizing protonated ethanol as reagent ions has been developed to simultaneously detect atmospheric gaseous amines (C_1 to C_6) and amides (C_1 to C_6). ~~Protonated ethanol was selected as the reagent ions because the higher~~ proton affinity of ethanol ($185.6 \text{ kcal mol}^{-1}$) is higher than that of water ($165.2 \text{ kcal mol}^{-1}$), as shown in Table 1, ~~resulting~~ in more selectivity for detecting high proton affinity species (*e.g.* $> 196 \text{ kcal mol}^{-1}$ for amines and amides) (Nowak, 2002; Yu and Lee, 2012; You et al., 2014). The influences of RH and organics on amine and amide detection were characterized in the laboratory. Ambient measurements of amines and amides utilizing this method were performed from 25 July 2015 to 25 August 2015 in urban Shanghai, China. During the campaign, a Filter Inlet for Gases and AEROsols (FIGAERO) was interfaced to HR-ToF-CIMS (Lopez-Hilfiker et al., 2014) but only results on gaseous C_1 - C_6 amines and amides are presented. The potential sources and sinks of amines and amides are discussed.

2 Experimental

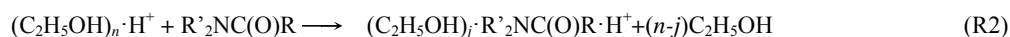
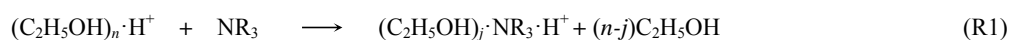
2.1 Instrumentation

An Aerodyne HR-ToF-CIMS (Bertram et al., 2011) with protonated ethanol as reagent ions has been deployed to detect gaseous amines (C_1 to C_6) and amides (C_1 to C_6). Protonated ethanol reagent

ions were generated by passing a pure air flow of 1 L min⁻¹ (liter per minute) supplied by a zero air generator (Aadco 737) through a Pyrex bubbler containing ethanol ($\geq 96\%$, J.T.Baker) and then through a 0.1 mCi ²⁴¹Am radioactive source. A sample flow of 1.35 L min⁻¹ was introduced into the ion-~~molecular-molecule~~ reaction (IMR) chamber where the sample flow and the reagent ion flow converge. The pressures of the IMR chamber and the small-segmented quadrupole (SSQ) were regulated at ~ 100 mbar and ~ 2.8 mbar, respectively, to increase the instrument sensitivity. Under such conditions, the ion-~~molecular-molecule~~ reaction time was ~ 320 ms in the IMR. To minimize wall-loss of analytes on the inner surface of IMR, the temperature of IMR was maintained at an elevated temperature (50°C). The data of HR-ToF-CIMS was collected at 1 Hz time resolution.

Under dry conditions, the most abundant reagent ion was the protonated ethanol dimer ((C₂H₅OH)₂·H⁺, m/z 93.0910), with the ~~second most next~~ dominant ions being the protonated ethanol monomer ((C₂H₅OH)·H⁺, m/z 47.0491) and the protonated ethanol trimer ((C₂H₅OH)₃·H⁺, m/z 139.1329). The presence of water led to formation of clusters of protonated ethanol with water (C₂H₅OH·H₂O·H⁺) and hydronium ions and their hydrates ((H₂O)_n·H⁺, $n=1, 2$ and 3). A typical mass spectrum under $< 20\%$ RH is shown in Figure S1. The ratios of the oxygen cation (O₂⁺), the clusters of protonated ethanol with water (C₂H₅OH·H₂O·H⁺), and hydronium ions ((H₂O)_n·H⁺, $n=1, 2$ and 3) to the sum of (C₂H₅OH)·H⁺, (C₂H₅OH)₂·H⁺, and (C₂H₅OH)₃·H⁺ were ~ 0.001 , ~ 0.026 , and ~ 0.011 , respectively.

Amines and amides reacted dominantly with protonated ethanol ions ((C₂H₅OH)_n·H⁺, $n=1, 2$ and 3), compared to water clusters, with the formation of protonated amines/amides clustering with up to one molecule of ethanol, through proton transfer reactions. The ion-~~molecular-molecule~~ reactions of amines (denoted as NR₃, with R being either a hydrogen atom=H or an alkyl group) and amides (denoted as R'₂NC(O)R, with R' being either a hydrogen atom=H or an alkyl group) with protonated ethanol reagent ions can be represented by the following reactions~~showed as the following~~ (You et al., 2014; Yu and Lee, 2012):



where $n = 1, 2$, and 3 , and $j = 0$ and 1 .

2.2 Calibration of amines and amides

Amines and amides were calibrated using permeation sources. Permeation tubes for amines (methylamine (MA), dimethylamine (DMA), trimethylamine (TMA), and diethylamine (DEA)) were purchased from VICI Inc. USA, whereas those for amides (formamide (FA), $\geq 99.5\%$, GC, Sigma Aldrich; acetamide (AA), $\geq 99\%$, GC, Sigma Aldrich; and propanamide (PA), $\geq 96.5\%$, GC, Sigma Aldrich) were home-made using 1/4 inch Teflon tubes with the ends sealed with Teflon blockers. The permeation tube was placed in a U-shape glass tube with a diameter of 2.5 cm that was immersed in a liquid bath with precise temperature regulation (Zheng et al., 2015). A high purity ($\geq 99.999\%$) nitrogen flow typically at 0.1 L min^{-1} was used as the carrier gas to carry the permeated compounds to HR-ToF-CIMS for detection.

The concentration of an amine in the outflow of the permeation tube was ~~referred to that as~~ determined by an acid-base titration method (Freshour et al., 2014). The high purity nitrogen flow containing an amine standard was bubbled through a HCl solution ($\text{pH} \approx 4.5$) with a small amount of KCl ($\sim 5 \text{ mM}$) added to facilitate measurements of pH values. Reagents HCl ($\sim 37 \text{ wt\%}$ in water) and KCl ($\geq 99\%$) were of ACS reagents and purchased from Sigma Aldrich. The concentration of the amine was derived according to variations of the pH values with titration time. The pH values were averaged and recorded by a pH meter (340i, WTW, Germany) every 5 min.

In the case of amides, a permeated alkyl-amide was trapped in a HNO_3 solution with a pH of ~ 2.5 that was diluted from reagent HNO_3 ($\sim 70 \text{ wt\%}$ in water, ACS reagent, Sigma Aldrich). Hydrolysis of the alkyl-amide occurred under acidic conditions leading to formation of NH_4^+ (Cox and Yates, 1981). The concentration of NH_4^+ was quantified using Ion Chromatography (Metrohm 833, Switzerland), and the permeation rate of the alkyl-amide was derived from the variation of NH_4^+ with the time period of hydrolysis.

~~The total ethanol reagent ion signals, i.e., the sum of the protonated ethanol monomer, dimer, and trimer, during the laboratory calibration were typically $\sim 0.32 \text{ MHz}$, which yields a small correction because of the variation in total reagent ions between in laboratory calibration and during field measurements as stated in section 2.4. The total ethanol reagent ion signals during the laboratory calibration were typically $\sim 0.32 \text{ MHz}$.~~

2.3 Influence of RH and organics

Experiments were performed to characterize the influence of RH and organics on the detection of

amines and amides. The schematics of our experimental setup are shown in Figure S2 (A for tests at elevated RH and B for tests in presence of organics), where the tubes and valves are made of polytetrafluoroethylene (PTFE) and perfluoroalkoxy (PFA) materials to minimize absorption of amines/amides on the inner surface of tubes and valves. To examine the influence of RH, a pure air flow was directed through a bubbler filled with 18.2 M Ω -cm deionized water, and then mixed with the amine/amide flow of 0.1 L min⁻¹ generated from the permeation sources. The examined RH ranged from 4 % to 65%.

α -pinene, a typical biogenic organic compound, and p-xylene, a typical anthropogenic compound, were chosen to examine the influence of organics on detection of amines and amides. The amines/amide flow was mixed with organics for \sim 0.2 s before entering the IMR. During the characterization, the air flow (15 L min⁻¹) containing α -pinene or p-xylene with concentrations up to ~~hundreds of 200 ppbv (parts per billion by volume)~~ was initially mixed with the amine/amide flow of 0.1 L min⁻¹ generated from the permeation sources. Then ozone and OH radicals were generated from an O₂/H₂O flow of 2×10^{-3} L min⁻¹ by turning on a Hg-lamp (Jelight model 600, USA). Photochemical reactions of α -pinene or p-xylene occurred and a much more complex mixture of organics was subsequently mixed with the amine/amide flow.

2.4 Field campaign in urban Shanghai

The ethanol HR-ToF-CIMS was deployed for a field campaign at the Fudan site (31° 17' 54" N, 121° 30' 05" E) on the campus of Fudan University from 25 July through 25 August, 2015. This monitoring site is on the rooftop of a teaching building that is \sim 20 m above ground. About 100 m to the north is the Middle Ring that is one of the main overhead highways in Shanghai. This site is also influenced by local industrial and residential activities. Hence, the Fudan site is a representative urban site (Ma et al., 2014; Wang et al., 2013a; Wang et al., 2016; Xiao et al., 2015).

The schematic of the ethanol HR-ToF-CIMS setup during the field campaign is shown in Figure S3. Ambient air was drawn into a PTFE tubing with a length of 2 m and an inner diameter of 3/8 inch. To minimize the wall-loss of amines and amides, a high sampling flow rate (15 L min⁻¹) was adopted, resulting in an inlet residence time of \sim 0.26 s. Also, the PTFE tubing was heated to 50°C by heating tapes. Because of the high concentrations of volatile organic compounds in the air of urban Shanghai, reagent ion depletion occurred during the initial tests of measurements of ambient samples. Hence, the

ambient air was diluted with a high purity nitrogen flow with a dilution ratio of ~1:4.6. Under such condition, variation of the total reagent ions ($(\text{C}_2\text{H}_5\text{OH})\cdot\text{H}^+$, $(\text{C}_2\text{H}_5\text{OH})_2\cdot\text{H}^+$, and $(\text{C}_2\text{H}_5\text{OH})_3\cdot\text{H}^+$) was less than 10% between measurements of the background air and the ambient sample. The ethanol reagent ion signals were typically around 0.35 MHz throughout the entire campaign. To take the variation in total reagent ions between in laboratory calibration and during field measurements into account, ambient concentrations of amines and amides were calculated according to

$$[\text{amines or amides}]_{\text{ambient}} = C_{\text{amines or amides}} \times \frac{\sum_{n=0-1}(\text{amines or amides})\cdot(\text{C}_2\text{H}_5\text{OH})_n\cdot\text{H}^+}{\sum_{n=1-3}(\text{C}_2\text{H}_5\text{OH})_n\text{H}^+} \quad (1)$$

where C is a calibration coefficient obtained by dividing the total reagent ion signals in laboratory calibration by the sensitivity of an amine or amide. As shown in equation (1), to minimize the effect of the variation of reagent ions during field measurements, the ambient signals of an amine or amide were normalized by the sum of ethanol clusters including the protonated ethanol monomer, dimer, and trimer.

During the campaign, a Filter Inlet for Gases and AEROSols (FIGAERO) (Lopez-Hilfiker et al., 2014) was attached to the HR-ToF-CIMS. FIGAERO-HRToF-CIMS offers two operation modes. Direct gas sample analysis occurs with the HR-ToF-CIMS during simultaneous particle collection on a PTFE filter via a separate dedicated port. Particle analysis occurs via evaporation from the filter using temperature-programmed thermal desorption by heated ultra-high purity nitrogen upstream of the HR-ToF-CIMS. A moveable filter housing automatically switches between the two modes. In our study, measurements of ambient gaseous samples were conducted for 20 min every hour, followed by analysis of particulate samples for 40 min. In this paper, we focus on measurements of gaseous samples and present results on detection of gaseous amines and amides.

During the 20 min period for analysis of ambient gaseous samples, background measurements were auto-performed for 5 min by a motor-driven three-way Teflon solenoid valve, utilizing a high purity nitrogen flow as the background gas. Figure S4 shows typical background signals during an ambient sampling period of 3 h. The average ambient background concentrations of amines (C_1 to C_6) and amides (C_1 to C_6) throughout the field campaign are presented in Table 1. The inlet memory of amines and amides were determined using an inlet spike approach. As shown in Figure S5, the signals followed the sum of two decaying exponentials. The characteristic decaying times of two exponentials, which are displacement of amines and amides inside the inlet by pumping and removing amines and

amides adsorbed on the inlet surface (Zheng et al., 2015), were 1.1 s and 8.5 s for TMA, and 1.4 s and 1.4 s for PA, respectively. These results demonstrate that a 5 min background sampling time is sufficient to eliminate the inlet memory.

All HR-ToF-CIMS data were analyzed with Tofware (Aerodyne Research, Inc. and ToFwerk AG) and Igor Pro (Wavemetrics) software. Concentrations of O₃ were measured by an O₃ analyzer (Model 49i, Thermo Scientific, USA). RH and temperature were measured by an automatic meteorological station (CAWS600, Huayun, China) at the Fudan site.

Solar radiation intensity measured by a pyranometer (Kipp & Zonen CMP6, Netherlands) was obtained from the Shanghai Pudong Environmental Monitoring Centre (31°14' N, 121°32' E, about 8.78 km from the Fudan site). Precipitation was recorded by a rainfall sensor (RainWise Inc., USA) located at the Huangxing Park monitoring station (31°17' N, 121°32' E, about 2.95 km from the Fudan site) of Shanghai Meteorology Bureau.

3 Results and Discussion

3.1 Performance of ethanol HR-ToF-CIMS in the laboratory

3.1.1 Sensitivities and detection limits

The permeation rates of amines and amides were determined adopting methods of acid-base titration and hydrolysis of alkyl-amides in an acidic solution, respectively. A typical plot for determination of the permeation rate of the DEA permeation tube is shown in Figure S6. Plots for FA (C₁-amide) and PA (an isomer of C₃-amide) are used as examples for amides, as shown in Figure S7. In summary, at 0°C, the permeation rates of MA, DMA, TMA, and DEA permeation tubes were 6.9 ± 0.7 , 7.4 ± 0.2 , 5.1 ± 0.8 , and 12.7 ± 0.9 ng min⁻¹, respectively. Permeation rates of home-made FA, AA, and PA permeation tubes were 36.7 ± 2.4 , 5.2 ± 0.5 , and 29.1 ± 1.6 ng min⁻¹, respectively, at 0°C.

The high purity nitrogen flow carrying the permeated amine/amide was then diluted with another high purity nitrogen flow at different dilution ratios, and directed to HR-ToF-CIMS for detection under dry conditions (RH = ~ 0%). Figure S8 shows the calibration curves of C₁- to C₄-amines and C₁- to C₃-amides. The derived sensitivities were 5.6-19.4 Hz pptv⁻¹ for amines and 3.8-38.0 Hz pptv⁻¹ for amides with the total reagent ions of ~0.32 MHz, respectively. Also, the detection limits of amines and amides were 0.10-0.50 pptv and 0.29-1.95 pptv at 3σ of the background signal for a 1-min

integration time, respectively. Sensitivities, calibration coefficients, and detection limits of the C₁- to C₄-amines (MA, DMA, TMA, and DEA) and C₁- to C₃-amides (FA, AA, and PA), together with their proton affinities, are summarized in Table 1. The detection limits of C₁- to C₃-amines in our study are similar to those by Zheng et al. (2015) and You et al. (2014). The sensitivities of C₁- to C₄-amines are slightly better than those reported in You et al. (2014) and Yu and Lee (2012).

3.1.2 Effects of RH and organics

The presence of high concentrations of water is believed to have an effect on the ion-molecule reactions in IMR, given the proton transfer nature of our ion-molecule reactions and the high IMR pressure (providing longer ion-molecule reaction time) in our study. The detection of constant concentrations of amines and amides by HR-ToF-CIMS at various RH was characterized to evaluate the influence of RH. Examined were MA (C₁-amine) and TMA (C₃-amine) under 0-65% RH at 23°C, corresponding to 0-70% and 0-49% enhancement in the MS signal, respectively. In the case of amides, the increase of the PA (C₃-amide) signal was 0-38% under 0-55% RH. These results show that RH has an obvious effect on the MS signals for amines and amides, which followed sigmoidal fits with $R^2 \geq 0.97$ in the examined RH range (Figure 1).

At elevated RH, high concentrations of water resulted in the production of (H₂O)_mH⁺ (m=1,2 and 3) and C₂H₅OH·H₂O·H⁺ ions (Figure S1) (Nowak et al., 2002). Proton transfer reactions of (H₂O)_mH⁺ (m=1,2 and 3) and C₂H₅OH·H₂O·H⁺ with amines and amides might occur leading to the formation of additional protonated amines and amides. In addition, the proton affinities of amines are generally higher than those of amides. Thus, the relative enhancement was more significant for amines.

Since a large number of ambient organics can be detected by this protonated ethanol reagent ion methodology as shown later, laboratory measurements of amines and amides in presence of and in absence of organics formed from photo oxidation of α-pinene and p-xylene, respectively, were carried out to examine the influence of organics on detection of amines and amides. Figure 2 shows the effects of biogenic (α-pinene) and anthropogenic (p-xylene) compounds and their photochemical reaction products on detection of amines (MA and TMA) and amide (PA) by our HR-ToF-CIMS. After stable signals of amines/amide were established, introduction of α-pinene and p-xylene, respectively, had little impact on detection of amines and amides. Initiation of photochemical reactions of α-pinene and p-xylene upon turning on the Hg-lamp, as evidenced by characteristic

products of pinonaldehyde from α -pinene (Lee et al., 2006) and 3-hexene-2,5-dione from p-xylene (Smith et al., 1999), respectively, did not have an obvious effect on detection of amines and amides, either.

3.2 Detection of amines and amides in urban Shanghai

3.2.1 Identification of nitrogen-containing species

One major challenge during analysis of mass spectra from the field deployment of the ethanol HR-ToF-CIMS is to distinguish amines and amides with very close m/z values in order to achieve simultaneous measurements. Thanks to the high mass resolving power ($R \geq 3500$ in V-mode) of our HR-ToF-CIMS, we are able to distinguish and identify the following protonated amines ($\text{CH}_5\text{N}\cdot\text{H}^+$ (m/z 32.0495), $\text{C}_2\text{H}_7\text{N}\cdot\text{H}^+$ (m/z 46.0651), $\text{C}_3\text{H}_9\text{N}\cdot\text{H}^+$ (m/z 60.0808), $\text{C}_4\text{H}_{11}\text{N}\cdot\text{H}^+$ (m/z 74.0964), $\text{C}_5\text{H}_{13}\text{N}\cdot\text{H}^+$ (m/z 88.1121), and $\text{C}_6\text{H}_{15}\text{N}\cdot\text{H}^+$ (m/z 102.1277)), and amides ($\text{CH}_3\text{NO}\cdot\text{H}^+$ (m/z 46.0287), $\text{C}_2\text{H}_5\text{NO}\cdot\text{H}^+$ (m/z 60.0444), $\text{C}_3\text{H}_7\text{NO}\cdot\text{H}^+$ (m/z 74.0600), $\text{C}_4\text{H}_9\text{NO}\cdot\text{H}^+$ (m/z 88.0757), $\text{C}_5\text{H}_{11}\text{NO}\cdot\text{H}^+$ (m/z 102.0913), and $\text{C}_6\text{H}_{13}\text{NO}\cdot\text{H}^+$ (m/z 116.1069)), as well as a few ~~oxamides~~~~oxemides~~ ($\text{C}_3\text{H}_5\text{NO}_2\cdot\text{H}^+$ (m/z 88.0393), $\text{C}_4\text{H}_7\text{NO}_2\cdot\text{H}^+$ (m/z 102.0550), and $\text{C}_5\text{H}_7\text{NO}_2\cdot\text{H}^+$ (m/z 116.0760)), as shown by the single peak fitting for each of them in Figure 3. The assignment of molecular formulas for these species is within a mass tolerance of < 10 ppm, and the fitted area ranges from 99% to 101%.

We further analyzed the entire mass spectra and assigned a molecular formula to ~~202200~~ species with m/z values less than 163 Th as listed in Table S1, which allows a mass defect plot for typical 15-min mass spectra in Figure 4A. In addition to the protonated C_1 to C_6 -amines and amides, the presence of their clusters with one ethanol ~~molecule is~~ evident, which—further ~~confirming~~ confirms the identification of these species. A number of gaseous amines have been previously detected in the ambient air utilizing quadrupole mass spectrometer (Freshour et al., 2014; Hanson et al., 2011; Sellegri et al., 2005; You et al., 2014; Yu and Lee, 2012). As suggested by Hanson et al. (2011), an amine and an amide with one less carbon might both have high enough proton affinities and could be detected at the same unit m/z value by a quadrupole mass spectrometer, leading to uncertainty in measuring the ambient amine. In this study, C_1 - to C_6 -amines and C_1 - to C_6 -amides are, for the first time, systematically and simultaneously detected in ambient air.

In addition to the protonated C_1 to C_6 -amines and C_1 to C_6 -amides and their clusters with ethanol,

we were able to detect many other nitrogen-containing species (*e.g.* ammonia). Among the ~~200-202~~ species with m/z less than 163 Th, there were 86 nitrogen-containing species (Figure 4B and Table S1). Four imines (or enamines) including CH₃N, C₂H₅N, C₃H₇N, and C₄H₉N were detected. These imines (or enamines) could derive from photo-oxidation of amines (Nielsen et al., 2012) and play important roles in atmospheric processes (Bunkan et al., 2014). In addition, a number of heterocyclic nitrogen-containing species including pyrrole, pyrroline, pyrrolidine, pyridine, and pyrimidine were potentially detected (see Table S1). Berndt et al. (2014) reported that pyridine was able to enhance nucleation in H₂SO₄/H₂O system. Also, proton affinities of most of these heterocyclic nitrogen-containing compounds are higher than that of ammonia, hence they potentially have the capacity to neutralize atmospheric acidic species (*e.g.* H₂SO₄, HNO₃ and organic acids) to contribute to secondary particle formation and growth.

Apart from clusters of ammonia, C₁- to C₆-amines, and C₁- to C₆-amides with water or ethanol, there were forty-eight C_aH_bN_cO_d species representing 55.8 % of the total nitrogen-containing species. This suggests that more than half of the nitrogen-containing species existed as oxygenated compounds in the atmosphere in urban Shanghai. One important atmospheric nitrogen-containing compound isocyanic acid (HNCO) (Roberts et al., 2011) is not listed in Table S1, because the proton affinity of isocyanic acid is 180.0 kcal mol⁻¹, which is less than that of ethanol (185.6 kcal mol⁻¹). Hence, the ethanol reagent ions are not sensitive to the detection of isocyanic acid.

The rest ~~114-116~~ species with m/z less than 163 Th are mostly organics (see Table S1). Above $m/z=163$ Th, numerous mass peaks were observed, which are likely organics and nitrogen-containing species. These high-molecular-weight species are assumed to have a low volatility and may partition between the gas phase and the particles.

3.2.2 Time profiles of amines and amides

During the field measurement, the average RH of the diluted gaseous samples was 15.8±3.5%. According to our laboratory characterization, the MS signals of MA, TMA, and PA at 15.8% RH have been in average enhanced by 10%, 9%, and 19%, respectively, from our calibration under dry condition. Here, we use our sigmoidal fits to convert each of our ambient data points to the signal under dry condition (RH = ~0%), and calculate the corresponding concentration. Since MA and TMA behaved quite similarly at elevated RH, the sigmoidal fit for TMA is also applied to the C₂-amines and

C₄- to C₆-amines. Also, the sigmoidal fit for PA is adopted for other amides. Since high purity nitrogen (RH = ~0%) was used as the background sample during the ambient campaign, no RH-dependent correction was made with background signals.

Assuming C₁- to C₄-amines have the same proton affinity as MA, DMA, TMA, and DEA, respectively, the sensitivities of MA, DMA, TMA, and DEA were used to quantify C₁- to C₄-amines. Since the sensitivities of C₅- to C₆-amine standards were not determined~~are unavailable~~, the sensitivity of DEA by HR-ToF-CIMS was adopted to quantify C₅- to C₆-amines. A similar approach was utilized to quantify C₁- to C₃-amides by sensitivities of FA, AA, and PA, respectively. In addition, the sensitivity of PA was used to quantify C₄- to C₆-amides.

Figure 5 presents the time profiles for mixing ratios of C₁- to C₆-amines and C₁- to C₆-amides, respectively, from 25 July to 25 August 2015 in urban Shanghai. Note that each ~~date-data~~ point in the figure represents an average of 15-min measurements. Table 2 and Table 3 summarizes the mean concentrations of C₁- to C₆-amines and C₁- to C₆-amides throughout the entire campaign, together with comparison of amine and amide concentrations reported in previous field studies.

For C₁- to C₆-amines, the average concentrations ($\pm\sigma$) were 15.7 \pm 5.9 pptv, 40.0 \pm 14.3 pptv, 1.1 \pm 0.6 pptv, 15.4 \pm 7.9 pptv, 3.4 \pm 3.7 pptv, and 3.5 \pm 2.2 pptv, respectively. C₁-amine, C₂-amines, and C₄-amines were the dominant amine species in urban Shanghai. The concentrations of amines in Shanghai are generally smaller than those in Hyytiälä, Finland (Hellén et al., 2014; Kieloaho et al., 2013; Sellegri et al., 2005), except for one study that, as stated by the authors, should be treated with caution (Sipilä et al. 2015), potentially hinting that sources for amines existed in the forest region of Hyytiälä, Finland. Our C₁- and C₂-amines are generally more abundant than those in agricultural, coastal, continental, suburban, and urban areas (Freshour et al., 2014; Hanson et al., 2011; Kieloaho et al., 2013; Kürten et al., 2016; Sellegri et al., 2005; You et al., 2014). However, our C₃- to C₆-amines are less, potentially because we are able to distinguish an amine, an amide with one less carbon, and an ~~oxe~~amide with two less carbons (see Figure 3).

For C₁- to C₆-amides, the average concentrations ($\pm\sigma$) were 2.3 \pm 0.7 pptv, 169.2 \pm 51.5 pptv, 778.2 \pm 899.8 pptv, 167.8 \pm 97.0 pptv, 34.5 \pm 13.3 pptv, and 13.8 \pm 5.2 pptv, respectively. C₂-amides, C₃-amides, and C₄-amides were the most abundant amides in urban Shanghai during the campaign

and their concentrations were up to hundreds of pptv. ~~Especially, the concentration of C₃-amides reached ~8700 pptv.~~ Up to now, studies that report systematical identification and quantification of amides in the ambient air are lacking. Leach et al. (1999) detected *N,N*-dimethylformamide (an isomer of C₃-amides) of 368-4357 pptv in a suburban area surrounded by municipal incinerator, waste collection and processing center, and sewage treatment plant. In the ambient air, C₁- to C₆-amides may derive from oxidation of C₁- to C₆-amines. *N,N*-dimethylformamide is a major product with a yield of ~40% from photolysis experiments of TMA under high NO_x conditions (Nielsen et al, 2011). Also, the yields of formamide (C₁-amide) and methylformamide (C₂-amide) from OH-initiated MA and DMA in the presence of NO_x are ~11% and ~13%, respectively (Nielsen et al, 2012). Comparison of the abundance of amines and amides during the campaign, together with the yields of amides from photo-oxidation of amines, suggests that the ambient C₁- to C₃-amines were insufficient to explain the observed abundance of C₁- to C₃-amides. Therefore, in addition to secondary sources, C₁- to C₆-amides likely were emitted from primary sources (*e.g.* industrial emissions).

Figure 6 shows a close examination on the temporal variations of C₂-amines and C₃-amides, representatives of the observed amines and amides, together with that of rainfall between 20 August 2015 and 25 August 2015. The plots clearly reveal that the concentrations of C₂-amines and C₃-amides on raining days were maintaining at low levels, much lower than those without rain, and that C₂-amines and C₃-amides rapidly went up after the rain. Previous studies reported that wet deposition is one of the important sinks of amines (Cornell et al., 2003; Ge et al., 2011a, b; You et al., 2014). Our study further indicates that wet deposition (or heterogeneous reactions) is also an important sink for amides.

3.2.3 Diurnal patterns

Figure 7 presents the averaged diurnal variations of C₁- and C₂-amines and C₃- and C₄-amides, together with those of temperature, radiation, and ozone concentration during the campaign. Diurnal patterns for amines and amides with less variation are exhibited in Figure S9. Mixing ratios of C₁- and C₂-amines and C₃- and C₄-amides reached their peak values in the early morning (6:00~7:00am), and then started to decline as the temperature increased. The mixing ratios were normally the lowest during the day when the temperature rose to the top. The diurnal behavior of amines and amides can be explained by the strong photochemical reactions of these species during the daytime (Barnes et al.,

2010; Borduas et al., 2015; Nielsen et al., 2012), especially in summer, as evidenced by the negative correlations between the mixing ratios and radiation (exponential fits with $-0.0002 \leq \text{exponents} \leq -0.0001$), and between the mixing ratios and ozone (exponential fits with $-0.003 \leq \text{exponents} \leq -0.001$), a tracer for photochemical activities. Also, nighttime chemistry of amines with NO_3 radicals could be active. In summer night time of Shanghai, the NO_3 radical concentration could be up to 10^{10} radicals cm^{-3} (Wang et al., 2013b) and the reaction rates of amines with NO_3 radicals are at the order of $10^{-13} \text{ cm}^3 \text{ molecular}^{-1} \text{ s}^{-1}$ (Nielsen et al., 2012). Hence, high mixing ratios of amines at nighttime could be a secondary source of amides through reactions of amines with NO_3 radicals.

In addition, an opposite tendency between the mixing ratios and the temperature (exponential fits with $-0.067 \leq \text{exponents} \leq -0.049$) is clearly evident in our study, which is in contrast to the positive temperature dependence of C_3 -amines and C_6 -amines in previous studies (Hanson et al., 2011; You et al., 2014; Yu and Lee, 2012). The positive temperature dependencies of C_3 -amines was explained by deposition of amines onto soil or grass landscape at night and then partitioning back to the atmosphere in the morning when the surface heats (Hanson et al., 2011; You et al., 2014). On the other hand, land surface in Shanghai is mainly covered by bitumen and cement, on which the behavior of amines might be different.

3.2.4 Source identification for C_3 -amides

A Lagrangian dispersion model has been utilized to further understand the potential sources of C_3 -amides. This Lagrangian modeling simulation is based on Hybrid Single-Particle Lagrangian Integrated Trajectory (HYSPPLIT) (Draxler and Hess, 1998; Stein et al., 2015) following the method developed by Ding et al. (2013). Three-day backward retroplumes (100 m above the ground level) from the Fudan sampling site are ~~shown~~ demonstrated for air masses with mixing ratios of C_3 -amides $> 2670 \text{ pptv}$ in Figure 8, and for air masses ~~with the C_3 -amide concentration range between 1340 pptv and 2650 pptv~~ with $2650 \text{ pptv} > \text{mixing ratios of } \text{C}_3\text{-amides} > 1340 \text{ pptv}$ in Figure S10, respectively. ~~Especially, in Figure 8 A, the concentration of C_3 -amides reached $\sim 8700 \text{ pptv}$.~~ The embedded 12 h retroplumes give a better view of the local zones through which the air masses with high concentrations of C_3 -amides passed before their arrival to the sampling site. Since the atmospheric lifetimes of *N,N*-dimethylformamide (an isomer of C_3 -amides) and its potential precursor TMA (an isomer of C_3 -amines) in respect to reactions with OH radicals are $\sim 3 \text{ h}$ and $\sim 10 \text{ h}$, respectively, using

an 12 h-average OH radical concentration of 2×10^6 radicals cm^{-3} , C_3 -amides were likely emitted or formed along the trajectory. As shown in Figure 8A-D, the air plumes with high concentrations of C_3 -amides mainly originated from the sea and came from the north of Shanghai. The air mass passed through predominantly industrial areas and cities after landing, and Baoshan industrial zone (one of the main industrial zones in Shanghai) was right on its path during the last 12 hours. Therefore, industrial emissions (or other anthropogenic emissions) might be important sources of C_3 -amides.

Figure S10A-E presents another five cases with the next highest concentrations of C_3 -amide. The air masses primarily came from southwest of the sampling site, and then passed through industrial areas and cities before arrival, including Songjiang and Jinshan industrial zones (another two main industrial zones in Shanghai) during the last 12 hours. These results also suggest that industrial emissions or other anthropogenic activities might be important sources of C_3 -amides.

4 Conclusions

This paper presents laboratory characterization of an ethanol HR-ToF-CIMS method for detection of amines and amides, and one month field deployment of the ethanol HR-ToF-CIMS in urban Shanghai during summer 2015. Laboratory characterization indicates that our sensitivities for amines (5.6-19.4 Hz pptv⁻¹) and amides (3.8-38.0 Hz pptv⁻¹) and detection limits for amines (0.10-0.50 pptv) and amides (0.29-1.95 pptv) at 3σ of the background signal for a 1-min integration time, respectively, are slightly better than those in previous studies using a similar protonated ethanol-CIMS methods (You et al., 2014; Yu and Lee, 2012). Correction of the mass signals of amines and amides are necessary at elevated RH because of the significant RH dependence of detection of amines and amides as observed in the laboratory. On the other hand, organics with high proton affinity are unlikely to pose an effect on the detection of amines and amides as long as their concentrations will not lead to reagent ion depletion.

High time resolution, highly sensitive and simultaneous measurements of amines (from a few pptv to hundreds of pptv) and amides (from tens of pptv to a few ppbv) have been achieved during the ambient campaign. Their diurnal profiles suggest that primary emissions could be important sources of amides in urban Shanghai, in addition to the secondary formation processes, and that photo-oxidation and wet deposition of amines and amides might be their main loss pathway.

86 nitrogen-containing species including amines and amides were identified with m/z less than 163 Th, 55.8% of which are oxygenated. This certainly indicates that the ethanol HR-ToF-CIMS method potentially has a much wider implication in terms of measuring atmospheric nitrogen-containing species. For example, imines (or enamines) and a number of heterocyclic nitrogen-containing compounds (*e.g.* pyridine and quinoline) (see Table S1) were potentially detected by this method. ~~Berndt et al. (2014) reported that pyridine was able to enhance nucleation in H_2SO_4/H_2O system. Also, proton affinities of most of these heterocyclic nitrogen-containing compounds are higher than that of ammonia, hence they potentially have the capacity to neutralize atmospheric acidic species (*e.g.* H_2SO_4 , HNO_3 and organic acids) to contribute to secondary particle formation and growth.~~

Nevertheless, the detection of amides in ambient air is consistent with the photochemical chemistry that has been previously studied in the laboratory (Barnes et al., 2010; Borduas et al., 2015; Bunkan et al., 2016; Nielsen et al., 2012). ~~The Compared with amines, acetamide has a very weak positive enhancement on nucleation capability of sulfuric acid (Glasoe et al., 2015). On the other hand, the~~ mixing ratios of amides were significantly higher than those of amines in urban Shanghai during our measurements. Since the newly formed nano-particles are likely highly acidic (Wang et al., 2010a), hydrolysis of amides will give rise to NH_4^+ in the particle, in addition to those formed through direct neutralization between gaseous ammonia and particulate sulfuric acid. Although significant progresses on the roles of ammonia and amines in the atmospheric nucleation have been made (Almeida et al., 2013; Kürten et al., 2014) and it has been shown that acetamide can only slightly enhance the nucleation rate of sulfuric acid (Glasoe et al., 2015), the exact contribution of amides during atmospheric nucleation and subsequent growth events is yet to be elucidated.

Acknowledgement

This study was financially supported by the National Natural Science Foundation of China (No. 21190053, 21222703, 21561130150, & 41575113), the Ministry of Science & Technology of China (2012YQ220113-4), and the Cyrus Tang Foundation (No. CTF-FD2014001). LW thanks the Royal Society-Newton Advanced Fellowship (NA140106).

References

- Almeida, J., Schobesberger, S., Kürten, A., Ortega, I. K., Kupiainen-Määttä, O., Praplan, A. P., Adamov, A., Amorim, A., Bianchi, F., Breitenlechner, M., David, A., Dommen, J., Donahue, N. M., Downard, A., Dunne, E., Duplissy, J., Ehrhart, S., Flagan, R. C., Franchin, A., Guida, R., Hakala, J., Hansel, A., Heinritzi, M., Henschel, H., Jokinen, T., Junninen, H., Kajos, M., Kangasluoma, J., Keskinen, H., Kupc, A., Kurtén, T., Kvashin, A. N., Laaksonen, A., Lehtipalo, K., Leiminger, M., Leppä, J., Loukonen, V., Makhmutov, V., Mathot, S., McGrath, M. J., Nieminen, T., Olenius, T., Onnela, A., Petäjä, T., Riccobono, F., Riipinen, I., Rissanen, M., Rondo, L., Ruuskanen, T., Santos, F. D., Sarnela, N., Schallhart, S., Schnitzhofer, R., Seinfeld, J. H., Simon, M., Sipilä, M., Stozhkov, Y., Stratmann, F., Tome, A., Tröstl, J., Tsagkogeorgas, G., Vaattovaara, P., Viisanen, Y., Virtanen, A., Vrtala, A., Wagner, P. E., Weingartner, E., Wex, H., Williamson, C., Wimmer, D., Ye, P., Yli-Juuti, T., Carslaw, K. S., Kulmala, M., Curtius, J., Baltensperger, U., Worsnop, D. R., Vehkamäki, H., and Kirkby, J.: Molecular understanding of sulphuric acid-amine particle nucleation in the atmosphere, *Nature*, 502, 359-363, 10.1038/nature12663, 2013.
- Barnes, I., Solignac, G., Mellouki, A., and Becker, K. H.: Aspects of the Atmospheric Chemistry of Amides, *ChemPhysChem*, 11, 3844-3857, 10.1002/cphc.201000374, 2010.
- Barsanti, K. C., and Pankow, J. F.: Thermodynamics of the formation of atmospheric organic particulate matter by accretion reactions - Part 3: Carboxylic and dicarboxylic acids, *Atmos. Environ.*, 40, 6676-6686, 10.1016/j.atmosenv.2006.03.013, 2006.
- Bertram, T. H., Kimmel, J. R., Crisp, T. A., Ryder, O. S., Yatavelli, R. L. N., Thornton, J. A., Cubison, M. J., Gonin, M., and Worsnop, D. R.: A field-deployable, chemical ionization time-of-flight mass spectrometer, *Atmos.Meas.Tech.*, 4, 1471-1479, 10.5194/amt-4-1471-2011, 2011.
- Berndt, T., Sipilä, M., Stratmann, F., Petäjä, T., Vanhanen, J., Mikkilä, J., Patokoski, J., Taipale, R., Mauldin III, R. L., and Kulmala, M.: Enhancement of atmospheric H₂SO₄/H₂O nucleation: organic oxidation products versus amines, *Atmos. Chem. Phys.*, 14, 751-764, 10.5194/acp-14-751-2014, 2014.
- [Berndt, T., Stratmann, F., Sipilä, M., Vanhanen, J., Petäjä, T., Mikkilä, J., Grüner, A., Spindler, G., Lee Mauldin III, R., Curtius, J., Kulmala, M., and Heintzenberg, J.: Laboratory study on new particle formation from the reaction OH + SO₂: influence of experimental conditions, H₂O vapour, NH₃ and the amine tert-butylamine on the overall process, *Atmos. Chem. Phys.*, 10, 7101-7116, doi:10.5194/acp-10-7101-2010, 2010.](#)
- Borduas, N., da Silva, G., Murphy, J. G., and Abbatt, J. P.: Experimental and theoretical understanding of the gas phase oxidation of atmospheric amides with OH radicals: kinetics, products, and mechanisms, *J. Phys.Chem. A*, 119, 4298-4308, 10.1021/jp503759f, 2015.
- [Bunkan, A. J. C., Tang, Y. Z., Sellevag, S. R., and Nielsen, C. J.: Atmospheric Gas Phase Chemistry of CH₂=NH and HNC. A First-Principles Approach, *J. Phys.Chem. A*, 118, 5279-5288, 10.1021/jp5049088, 2014.](#)
- Bunkan, A. J. C., Mikoviny, T., Nielsen, C. J., and Wisthaler, A.: Experimental and theoretical study of the OH-initiated photo-oxidation of formamide, *J. Phys.Chem. A*, 120, 1222-1230, 10.1021/acs.jpca.6b00032, 2016.
- [Bzdek, B. R., Ridge, D. P., and Johnston, M. V.: Amine exchange into ammonium bisulfate and ammonium nitrate nuclei, *Atmos. Chem. Phys.*, 10, 3495-3503, doi:10.5194/acp-10-3495-2010, 2010.](#)
- [Cape, J. N., Cornell, S. E., Jickells, T. D., and Nemitz, E.: Organic nitrogen in the atmosphere — Where does it come from? A review of sources and methods, *Atmos. Res.*, 102, 30-48, 10.1016/j.atmosres.2011.07.009, 2011.](#)
- [Cheng, Y.; Li, S.; Leithead, A.:Chemical Characteristics and Origins of Nitrogen-Containing Organic Compounds in PM_{2.5} Aerosols in the Lower Fraser Valley, *Environ. Sci. Technol.*, 40, 5846-5852, 10.1021/es0603857, 2006.](#)

- Cornell, S. E., Jickells, T. D., Cape, J. N., Rowland, A. P., and Duce, R. A.: Organics nitrogen deposition on land and coastal environments: a review of methods and data, *Atmos. Environ.*, 37, 2173-2191, 10.1016/S1352-2310(03)00133-X, 2003.
- Cox, R. A., and Yates, K.: The hydrolyses of benzamides, methylbenzimidatium ions, and lactams in aqueous sulfuric-acid - the excess acidity method in the determination of reaction-mechanisms, *Can. J. Chem.*, 59, 2853-2863, Doi 10.1139/V81-414, 1981.
- [Dawson, M. L., Perraud, V., Gomez, A., Arquero, K. D., Ezell, M. J., and Finlayson-Pitts, B. J.: Measurement of gas-phase ammonia and amines in air by collection onto an ion exchange resin and analysis by ion chromatography, *Atmos. Meas. Tech.*, 7, 2733-2744, 10.5194/amt-7-2733-2014, 2014.](#)
- Draxler, R.R., and Hess, G.D.: An overview of the HYSPLIT_4 modeling system of trajectories, dispersion, and deposition. *Aust. Meteor. Mag.*, 47, 295-308, 1998.
- Ding, A. J., Wang, T., and Fu, C. B.: Transport characteristics and origins of carbon monoxide and ozone in Hong Kong, South China, *J. Geophys. Res. Atmos.*, 118, 9475-9488, 10.1002/jgrd.50714, 2013.
- El Dib, G., and Chakir, A.: Temperature-dependence study of the gas-phase reactions of atmospheric NO₃ radicals with a series of amides, *Atmos. Environ.*, 41, 5887-5896, 10.1016/j.atmosenv.2007.03.038, 2007.
- Erupe, M. E., Viggiano, A. A., and Lee, S. H.: The effect of trimethylamine on atmospheric nucleation involving H₂SO₄, *Atmos. Chem. Phys.*, 11, 4767-4775, 10.5194/acp-11-4767-2011, 2011.
- Finlayson-Pitts, B. J., and Pitts, J. N.: Chemistry of the upper and lower atmosphere : theory, experiments, and applications, Academic Press, San Diego, xxii, 969 p. pp., 2000.
- Freshour, N. A., Carlson, K. K., Melka, Y. A., Hinz, S., Panta, B., and Hanson, D. R.: Amine permeation sources characterized with acid neutralization and sensitivities of an amine mass spectrometer, *Atmos. Meas. Tech.*, 7, 3611-3621, 10.5194/amt-7-3611-2014, 2014.
- Glasoe, W. A., Volz, K., Panta, B., Freshour, N., Bachman, R., Hanson, D. R., McMurry, P. H., and Jen, C.: Sulfuric acid nucleation : an experimental study of the effect of seven bases, *J. Geophys. Res. Atmos.*, 120, 1933-1950, 10.1002/2014JD022730, 2015.
- Ge, X., Wexler, A. S., and Clegg, S. L.: Atmospheric amines – Part I. A review, *Atmos. Environ.*, 45, 524-546, 10.1016/j.atmosenv.2010.10.012, 2011.
- Hanson, D. R., McMurry, P. H., Jiang, J., Tanner, D., and Huey, L. G.: Ambient Pressure Proton Transfer Mass Spectrometry: Detection of Amines and Ammonia, *Environ. Sci. Technol.*, 45, 8881-8888, 10.1021/es201819a, 2011.
- Hellén, H., Kieloaho, A. J., and Hakola, H.: Gas-phase alkyl amines in urban air; comparison with a boreal forest site and importance for local atmospheric chemistry, *Atmos. Environ.*, 94, 192-197, 10.1016/j.atmosenv.2014.05.029, 2014.
- Kieloaho, A.-J., Hellén, H., Hakola, H., Manninen, H. E., Nieminen, T., Kulmala, M., and Pihlatie, M.: Gas-phase alkylamines in a boreal Scots pine forest air, *Atmos. Environ.*, 80, 369-377, 10.1016/j.atmosenv.2013.08.019, 2013.
- Kim, H. A., Kim, K., Heo, Y., Lee, S. H., and Choi, H. C.: Biological monitoring of workers exposed to N,N-dimethylformamide in synthetic leather manufacturing factories in Korea, *Int. Arch. Occup. Environ. Health*, 77, 108-112, 10.1007/s00420-003-0474-1, 2004.
- Kuhn, U., Sintermann, J., Spirig, C., Jocher, M., Ammann, C., and Neftel, A.: Basic biogenic aerosol precursors: Agricultural source attribution of volatile amines revised, *Geophys. Res. Lett.*, 38, L16811, doi:10.1029/2011GL047958, 2011.
- [Kupiainen, O., Ortega, I. K., Kurtén, T., and Vehkamäki, H.: Amine substitution into sulfuric acid – ammonia clusters, *Atmos. Chem. Phys.*, 12, 3591-3599, doi:10.5194/acp-12-3591-2012, 2012.](#)

625 Kürten, A., Jokinen, T., Simon, M., Sipilä, M., Sarnela, N., Junninen, H., Adamov, A., Almeida, J., Amorim, A.,
 626 Bianchi, F., Breitenlechner, M., Dommen, J., Donahue, N. M., Duplissy, J., Ehrhart, S., Flagan, R. C.,
 627 Franchin, A., Hakala, J., Hansel, A., Heinritzi, M., Hutterli, M., Kangasluoma, J., Kirkby, J., Laaksonen, A.,
 628 Lehtipalo, K., Leiminger, M., Makhmutov, V., Mathot, S., Onnela, A., Petäjä, T., Praplan, A. P., Riccobono,
 629 F., Rissanen, M. P., Rondo, L., Schobesberger, S., Seinfeld, J. H., Steiner, G., Tomé, A., Tröstl, J., Winkler,
 630 P. M., Williamson, C., Wimmer, D., Ye, P., Baltensperger, U., Carslaw, K. S., Kulmala, M., Worsnop, D. R.,
 631 and Curtius, J.: Neutral molecular cluster formation of sulfuric acid-dimethylamine observed in real time
 632 under atmospheric conditions, *Proc.Natl.Acad.Sci.*, 111, 15019-15024, 10.1073/pnas.1404853111, 2014.
 633 [Kürten, A., Bergen, A., Heinritzi, M., Leiminger, M., Lorenz, V., Piel, F., Simon, M., Sitals, R., Wagner, A., and](#)
 634 [Curtius, J.: Observation of new particle formation and measurement of sulfuric acid, ammonia, amines and](#)
 635 [highly oxidized molecules using nitrate CI-API-TOF at a rural site in central Germany. *Atmos. Chem. Phys.*](#)
 636 [Discuss.](#), doi:10.5194/acp-2016-294, in review, 2016.
 637 [Kurtén, T., Loukonen, V., Vehkamäki, H., and Kulmala, M.: Amines are likely to enhance neutral and](#)
 638 [ion-induced sulfuric acid-water nucleation in the atmosphere more effectively than ammonia, *Atmos. Chem.*](#)
 639 [Phys.](#), 8, 4095-4103, doi:10.5194/acp-8-4095-2008, 2008.
 640 [Laskin A, Smith J S, Laskin J. Molecular characterization of nitrogen-containing organic compounds in biomass](#)
 641 [burning aerosols using high-resolution mass spectrometry, *Environ. Sci. Technol.*, 43\(10\), 3764-3771,](#)
 642 [10.1021/es803456n, 2009.](#)
 643 Leach, J., Blanch, A., and Bianchi, A. C.: Volatile organic compounds in an urban airborne environment adjacent
 644 to a municipal incinerator, waste collection centre and sewage treatment plant, *Atmos. Environ.*, 33,
 645 4309-4325, Doi 10.1016/S1352-2310(99)00115-6, 1999.
 646 Lee, A., Goldstein, A. H., Kroll, J. H., Ng, N. L., Varutbangkul, V., Flagan, R. C., and Seinfeld, J. H.: Gas-phase
 647 products and secondary aerosol yields from the photooxidation of 16 different terpenes, *J. Geophys. Res.*
 648 *Atmos.*, 111, ArtId D1730510.1029/2006jd007050, 2006.
 649 Lee, D., and Wexler, A. S.: Atmospheric amines – Part III: Photochemistry and toxicity, *Atmos. Environ.*, 71,
 650 95-103, 10.1016/j.atmosenv.2013.01.058, 2013.
 651 Lopez-Hilfiker, F. D., Mohr, C., Ehn, M., Rubach, F., Kleist, E., Wildt, J., Mentel, T. F., Lutz, A., Hallquist, M.,
 652 Worsnop, D., and Thornton, J. A.: A novel method for online analysis of gas and particle composition:
 653 description and evaluation of a Filter Inlet for Gases and AEROSols (FIGAERO), *Atmos.Meas.Tech.*, 7,
 654 983-1001, 10.5194/amt-7-983-2014, 2014.
 655 Ma, Y., Xu, X., Song, W., Geng, F., and Wang, L.: Seasonal and diurnal variations of particulate organosulfates
 656 in urban Shanghai, China, *Atmos. Environ.*, 85, 152-160, 10.1016/j.atmosenv.2013.12.017, 2014.
 657 Malloy, Q. G. J., Qi, L., Warren, B., Cocker, D. R., Erupe, M. E., and Silva, P. J.: Secondary organic aerosol
 658 formation from primary aliphatic amines with NO₃ radical, *Atmos. Chem. Phys.*, 9, 2051-2060, 2009.
 659 Murphy, S. M., Sorooshian, A., Kroll, J. H., Ng, N. L., Chhabra, P., Tong, C., Surratt, J. D., Knipping, E., Flagan,
 660 R. C., and Seinfeld, J. H.: Secondary aerosol formation from atmospheric reactions of aliphatic amines,
 661 *Atmos. Chem. Phys.*, 7, 2313-2337, doi:10.5194/acp-7-2313-2007, 2007.
 662 Nielsen, C. J., Herrmann, H., and Weller, C.: Atmospheric chemistry and environmental impact of the use of
 663 amines in carbon capture and storage (CCS), *Chem. Soc. Rev.*, 41, 6684-6704, 10.1039/c2cs35059a, 2012.
 664 Nielsen, C. J., D'Anna, B., Karl, M., Aursnes, M., Boreave, A., Bossi, R., Bunkan, A. J. C., Glasius, M.,
 665 Hallquist, M., Hansen, A.-M. K., Kristensen, K., Mikoviny, T., Maguta, M. M., Müller, M., Nguyen, Q.,
 666 Westerlund, J., Salo, K., Skov, H., Stenström, Y., and Wisthaler, A.: Atmospheric Degradation of Amines
 667 (ADA), Norwegian Institute for Air Research, Kjeller, Norway, 2011.
 668 Nowak, J. B.: Chemical ionization mass spectrometry technique for detection of dimethylsulfoxide and

ammonia, *J. Geophys. Res. Atmos.*, 107, 10.1029/2001jd001058, 2002.

NIST: NIST Standard Reference Database Number 69, edited, National Institute for Standard Technology (NIST) Chemistry Web Book, available at: <http://webbook.nist.gov/chemistry/> (last access: 23 May 2016), 2016.

Qiu, C., Wang, L., Lal, V., Khalizov, A. F., and Zhang, R.: Heterogeneous reactions of alkylamines with ammonium sulfate and ammonium bisulfate, *Environ. Sci. Technol.*, 45, 4748-4755, 10.1021/es1043112, 2011.

[Roberts, J. M., Veres, P. R., Cochran, A. K., Warneke, C., Burling, I. R., Yokelson, R. J., Lerner, B., Gilman, J. B., Kuster, W. C., Fall, R., and de Gouw, J.: Isocyanic acid in the atmosphere and its possible link to smoke-related health effects, *Proc. Natl. Acad. Sci.*, 108, 8966-8971, 10.1073/pnas.1103352108, 2011.](#)

[Rogge, W. F., Hildemann, L. M., Mazurek, M. A., Cass, G. R., and Simonelt, B. R. T.: Sources Of Fine Organic Aerosol .1. Charbroilers And Meat Cooking Operations, *Environ. Sci. Technol.*, 25, 1112-1125, Doi 10.1021/Es00018a015, 1991.](#)

[Schmeltz, I., and Hoffmann, D.: Nitrogen-Containing Compounds In Tobacco And Tobacco-Smoke, *Chem. Rev.*, 77, 295-311, Doi 10.1021/Cr60307a001, 1977.](#)

Sellegrì, K., Hanke, M., Umann, B., Arnold, F., and Kulmala, M.: Measurements of organic gases during aerosol formation events in the boreal forest atmosphere during QUEST, *Atmos. Chem. Phys.*, 5, 373-384, 2005.

Smith, D. F., Kleindienst, T. E., and McIver, C. D.: Primary product distributions from the reaction of OH with m-, p-xylene, 1,2,4- and 1,3,5-trimethylbenzene, *J. Atmos. Chem.*, 34, 339-364, Doi 10.1023/A:1006277328628, 1999.

Smith, J. N., Barsanti, K. C., Friedli, H. R., Ehn, M., Kulmala, M., Collins, D. R., Scheckman, J. H., Williams, B. J., and McMurry, P. H.: Observations of aminium salts in atmospheric nanoparticles and possible climatic implications, *Proc. Natl. Acad. Sci.*, 107, 6634-6639, 10.1073/pnas.0912127107, 2010.

[Simon, M., Heinritzi, M., Herzog, S., Leiminger, M., Bianchi, F., Praplan, A., Dommen, J., Curtius, J., and Kürten, A.: Detection of dimethylamine in the low pptv range using nitrate chemical ionization atmospheric pressure interface time-of-flight \(CI-APi-TOF\) mass spectrometry, *Atmos. Meas. Tech.*, 9, 2135-2145, doi:10.5194/amt-9-2135-2016, 2016.](#)

[Sipilä, M., Sarnela, N., Jokinen, T., Junninen, H., Hakala, J., Rissanen, M. P., Praplan, A., Simon, M., Kürten, A., Bianchi, F., Dommen, J., Curtius, J., Petäjä, T., and Worsnop, D. R.: Bisulfate – cluster based atmospheric pressure chemical ionization mass spectrometer for high-sensitivity \(< 100 ppqV\) detection of atmospheric dimethyl amine: proof-of-concept and first ambient data from boreal forest, *Atmos. Meas. Tech.*, 8, 4001-4011, doi:10.5194/amt-8-4001-2015, 2015.](#)

Stein, A.F., Draxler, R.R., Rolph, G.D., Stunder, B.J.B., Cohen, M.D., and Ngan, F.: NOAA's HYSPLIT atmospheric transport and dispersion modeling system, *B. Am. Meteorol. Soc.*, 96, 2059-2077, doi:10.1175/BAMS-D-14-00110.1, 2015.

VandenBoer, T. C., Petroff, A., Markovic, M. Z., and Murphy, J. G.: Size distribution of alkyl amines in continental particulate matter and their online detection in the gas and particle phase, *Atmos. Chem. Phys.*, 11, 4319-4332, 10.5194/acp-11-4319-2011, 2011.

Wang, L., Khalizov, A. F., Zheng, J., Xu, W., Ma, Y., Lal, V., and Zhang, R.: Atmospheric nanoparticles formed from heterogeneous reactions of organics, *Nat. Geosci.*, 3, 238-242, 10.1038/ngeo778, 2010a.

Wang, L., Lal, V., Khalizov, A. F., and Zhang, R. Y.: Heterogeneous Chemistry of Alkylamines with Sulfuric Acid: Implications for Atmospheric Formation of Alkylaminium Sulfates, *Environ. Sci. Technol.*, 44, 2461-2465, 10.1021/es9036868, 2010b.

Wang, L., Du, H., Chen, J., Zhang, M., Huang, X., Tan, H., Kong, L., and Geng, F.: Consecutive transport of anthropogenic air masses and dust storm plume: Two case events at Shanghai, China, *Atmos. Res.*, 127,

713 22-33, 10.1016/j.atmosres.2013.02.011, 2013a.
 714 Wang, S., Shi, C., Zhou, B., Zhao, H., Wang, Z., Yang, S., and Chen, L.: Observation of NO₃ radicals over
 715 Shanghai, China, *Atmos. Environ.*, 70, 401-409, 10.1016/j.atmosenv.2013.01.022, 2013b.
 716 Wang, X. K., Rossignol, S., Ma, Y., Yao, L., Wang, M. Y., Chen, J. M., George, C., and Wang, L.: Molecular
 717 characterization of atmospheric particulate organosulfates in three megacities at the middle and lower
 718 reaches of the Yangtze River, *Atmos. Chem. Phys.*, 16, 2285-2298, 10.5194/acp-16-2285-2016, 2016.
 719 Xiao, S., Wang, M. Y., Yao, L., Kulmala, M., Zhou, B., Yang, X., Chen, J. M., Wang, D. F., Fu, Q. Y., Worsnop,
 720 D. R., and Wang, L.: Strong atmospheric new particle formation in winter in urban Shanghai, China, *Atmos.*
 721 *Chem. Phys.*, 15, 1769-1781, 10.5194/acp-15-1769-2015, 2015.
 722 You, Y., Kanawade, V. P., de Gouw, J. A., Guenther, A. B., Madronich, S., Sierra-Hernández, M. R., Lawler, M.,
 723 Smith, J. N., Takahama, S., Ruggeri, G., Koss, A., Olson, K., Baumann, K., Weber, R. J., Nenes, A., Guo,
 724 H., Edgerton, E. S., Porcelli, L., Brune, W. H., Goldstein, A. H., and Lee, S. H.: Atmospheric amines and
 725 ammonia measured with a chemical ionization mass spectrometer (CIMS), *Atmos. Chem. Phys.*, 14,
 726 12181-12194, 10.5194/acp-14-12181-2014, 2014.
 727 Yu, H., and Lee, S.-H.: Chemical ionisation mass spectrometry for the measurement of atmospheric amines,
 728 *Environ. Chem.*, 9, 190, 10.1071/en12020, 2012.
 729 Yu, H., McGraw, R., and Lee, S. H.: Effects of amines on formation of sub-3 nm particles and their subsequent
 730 growth, *Geophys. Res. Lett.*, 39, Art. L02807, 10.1029/2011gl050099, 2012.
 731 Zhang, R., Khalizov, A., Wang, L., Hu, M., and Xu, W.: Nucleation and growth of nanoparticles in the
 732 atmosphere, *Chem. Rev.*, 112, 1957-2011, 10.1021/cr2001756, 2012.
 733 Zheng, J., Ma, Y., Chen, M., Zhang, Q., Wang, L., Khalizov, A. F., Yao, L., Wang, Z., Wang, X., and Chen, L.:
 734 Measurement of atmospheric amines and ammonia using the high resolution time-of-flight chemical
 735 ionization mass spectrometry, *Atmos. Environ.*, 102, 249-259, 10.1016/j.atmosenv.2014.12.002, 2015.
 736 Zhu, L., Schade, G. W., and Nielsen, C. J.: Real-time monitoring of emissions from monoethanolamine-based
 737 industrial scale carbon capture facilities, *Environ. Sci. Technol.*, 47, 14306-14314, 10.1021/es4035045,
 738 2013.
 739

740 Table 1. Proton affinity, sensitivity, calibration coefficient, 1-min detection limit at 3σ of background signal during the laboratory characterization, and ambient
741 background of selected amines and amides.

Compounds	Proton affinity (kcal mol ⁻¹) (NIST, 2016)	Sensitivity (mean \pm σ) (Hz pptv ⁻¹) ^a	Calibration coefficient (10 ⁻² MHz Hz ⁻¹ pptv)	Detection limit (pptv)	Ambient background (mean \pm σ) (pptv) ^b
Water	165.2				
Ethanol	185.6				
Ammonia	204.0				
Methylamine (C ₁ -amine)	214.9	7.06 \pm 0.2	4.67	0.23	3.88 \pm 1.23
Dimethylamine (an isomer of C ₂ -amines)	222.2	5.6 \pm 0.2	5.89	0.50	6.64 \pm 1.24
Trimethylamine (an isomer of C ₃ -amines)	226.8	19.4 \pm 1.3	1.70	0.10	0.41 \pm 0.14
Diethylamine (an isomer of C ₄ -amines)	227.6	6.4 \pm 0.4	5.03	0.42	3.59 \pm 1.04
<i>N,N</i> -dimethyl-2-propanamine (an isomer of C ₅ -amines)	232.0				0.68 \pm 0.32
Triethylamine (an isomer of C ₆ -amines)	234.7				1.76 \pm 0.79
Formamide (an isomer of C ₁ -amide)	196.5	38.0 \pm 1.2	0.78	0.29	0.59 \pm 0.50
Acetamide (an isomer of C ₂ -amides)	206.4	3.8 \pm 0.3	7.89	0.45	8.63 \pm 3.63
<i>N</i> -methylformamide (an isomer of C ₂ -amides)	203.5				
Propanamide (an isomer of C ₃ -amides)	209.4	4.4 \pm 0.1	6.82	1.95	
<i>N</i> -methylacetamide (an isomer of C ₃ -amides)	212.4				59.76 \pm 48.37
<i>N,N</i> -dimethylformamide (an isomer of C ₃ -amides)	212.1				
<i>N</i> -ethylacetamide (an isomer of C ₄ -amides)	214.6				
<i>N,N</i> -dimethylacetamide (an isomer of C ₄ -amides)	217.0				13.59 \pm 10.01
2,2-dimethyl-propanamide (an isomer of C ₅ -amides)	212.5				8.47 \pm 5.18
<i>N,N</i> -dimethylbutyramide (an isomer of C ₆ -amides)	220.3				2.60 \pm 1.40

742

743 ^a Sensitivities were obtained under total reagent ion signals of \sim 0.32 MHz;

744 ^b Mean background values throughout the entire campaign \pm one standard deviation for C₁-to C₆-amines and C₁-to C₆-amides.

745 | Table 2 Inter-comparison of gaseous amines ~~and amides~~ measured in different locations with different surroundings.

746

	Location (site type, season)	C ₁ -Amine (pptv)	C ₂ -Amines (pptv)	C ₃ -Amines (pptv)	C ₄ -Amines (pptv)	C ₅ -Amines (pptv)	C ₆ -Amines (pptv)	C ₁ -Amide (pptv)	C ₂ -Amides (pptv)	C ₃ -Amides (pptv)	C ₄ -Amides (pptv)	C ₅ -Amides (pptv)	C ₆ -Amides (pptv)	Ref.
	Hyviiälä, Finland (Forested, Spring)	–	12.2±7.7 ^a	59±35.5 ^a										Sellegri et al.(2005)
	Hyviiälä, Finland (Forested, Summer- and Autumn)		157±20 ^b	102±61 ^b	15.5±0.5 ^b									Kieloaho et al.(2013)
	Hyviiälä, Finland (Forested, Summer)		39.1 ^a	10.2 ^a	8.1 ^a		1.6 ^a							Hellén et al.(2014)
	Alabama, USA (Forested, Summer)	<1.2	<4.8	1–10	<23.1	<17.3	<13.0							You et al. (2014)
	Ken., USA (Suburban, Winter)	<18	8 ± 3 ^a	16 ± 7 ^a	<41		<8							Yu and Lee (2012)
	Ken., USA (Suburban, Summer)	1.4	<4.4	5–10	10–50	10–100	<13.1							You et al. (2014)
	Southampton, UK (Suburban, Spring, Summer and Autumn)								368–4357					Leach et al.(1999)
	Lewis, USA (Coastal, Summer)	5 ^a	28 ^a	6 ^a	3 ^a	1 ^a	2 ^a							Freshour et al. (2014)
	Lansont, USA (Continental, Spring)	4 ^a	14 ^a	35 ^a	150 ^a	98 ^a	20 ^a							Freshour et al. (2014)
	Nanjing, China (Industrialized, Summer)	0.1–18.9	0.1–29.9	0.1–9.3										Zheng et al. (2014)
	Atlanta, USA (Urban, Summer)	<0.2	0.5–2	4–15	~5 ^d	4–5 ^d	3–25							Hanson et al. (2011)
	Helsinki, Finland (Urban, Summer)		23–6 ^a	8.4 ^a	0–3 ^a		0–1 ^a							Hellén et al.(2014)
	Toronto, Canada (Urban, Summer)		<2.7		<2.7		<1.0							VandenBoer et al.(2011)
	Shanghai, China (Urban, Summer)	15.7±5.9 ^a	40.0±14.3 ^a	1.1±0.6 ^a	15.4±7.9 ^a	3.4±3.7 ^a	3.5±2.2 ^a	2.3±0.7 ^a	169.2±51.5 ^a	778.2±899.8 ^a	167.8±97.0 ^a	34.5±13.3 ^a	13.8±5.2 ^a	This study
	<u>Location</u> (site type, season)		<u>C₁-Amine</u> (pptv)	<u>C₂-Amines</u> (pptv)	<u>C₃-Amines</u> (pptv)	<u>C₄-Amines</u> (pptv)	<u>C₅-Amines</u> (pptv)	<u>C₆-Amines</u> (pptv)						<u>Ref.</u>
	Hyviiälä, Finland (Forested, Spring)		–		12.2±7.7 ^a	59±35.5 ^a								Sellegri et al.(2005)
	Hyviiälä, Finland (Forested, Spring)				< 0.15									Sipilä et al. (2015)

<u>Hyytiälä, Finland (Forested,Summer and Autumn)</u>		<u>157±20^b</u>	<u>102±61^b</u>	<u>15.5±0.5^b</u>			<u>Kieloaho et al.(2013)</u>
<u>Hyytiälä, Finland (Forested,Summer)</u>		<u>39.1^c</u>	<u>10.2^c</u>	<u>8.1^c</u>		<u>1.6^c</u>	<u>Hellén et al.(2014)</u>
<u>Alabama, USA (Forested,Summer)</u>	<u>< 1.2</u>	<u>< 4.8</u>	<u>1-10</u>	<u>< 23.1</u>	<u>< 17.3</u>	<u>< 13.0</u>	<u>You et al. (2014)</u>
<u>Vielbrunn, Germany (Agricultural,Spring)</u>	<u>1-5</u>	<u>~1</u>	<u>1-5</u>	<u>1-5</u>		<u>1-5</u>	<u>Kürten et al. (2016)</u>
<u>Kent, USA (Suburban,Winter)</u>	<u>< 18</u>	<u>8 ± 3^a</u>	<u>16 ± 7^a</u>	<u>< 41</u>		<u>< 8</u>	<u>Yu and Lee. (2012)</u>
<u>Kent, USA (Suburban,Summer)</u>	<u>1-4</u>	<u>< 4.4</u>	<u>5-10</u>	<u>10-50</u>	<u>10-100</u>	<u>< 13.1</u>	<u>You et al. (2014)</u>
<u>Lewes, USA (Coastal,Summer)</u>	<u>5^c</u>	<u>28^c</u>	<u>6^c</u>	<u>3^c</u>	<u>1^c</u>	<u>2^c</u>	<u>Freshour et al. (2014)</u>
<u>Lamont, USA (Continental,Spring)</u>	<u>4^c</u>	<u>14^c</u>	<u>35^c</u>	<u>150^c</u>	<u>98^c</u>	<u>20^c</u>	<u>Freshour et al. (2014)</u>
<u>Nanjing, China (Industrialized,Summer)</u>	<u>0.1-18.9</u>	<u>0.1-29.9</u>	<u>0.1-9.3</u>				<u>Zheng et al. (2014)</u>
<u>Atlanta, USA (Urban,Summer)</u>	<u>< 0.2</u>	<u>0.5-2</u>	<u>4-15</u>	<u>~5^d</u>	<u>4-5^d</u>	<u>3-25</u>	<u>Hanson et al. (2011)</u>
<u>Helsinki, Finland (Urban,Summer)</u>		<u>23.6^c</u>	<u>8.4^c</u>	<u>0.3^c</u>		<u>0.1^c</u>	<u>Hellén et al.(2014)</u>
<u>Toronton, Canada (Urban,Summer)</u>		<u>< 2.7</u>		<u>< 2.7</u>		<u>< 1.0</u>	<u>VandenBoer et al.(2011)</u>
<u>Shanghai, China (Urban,Summer)</u>	<u>15.7±5.9^e</u>	<u>40.0±14.3^e</u>	<u>1.1±0.6^e</u>	<u>15.4±7.9^e</u>	<u>3.4±3.7^e</u>	<u>3.5±2.2^e</u>	<u>This study</u>

^a Mean values ± one standard deviation;

^b The highest concentrations during the measurement;

^c Mean values;

^d 8 h average values;

^e Mean values throughout the entire campaign ± one standard deviation.

Table 3 Inter-comparison of gaseous amides measured in different locations with different surroundings.

<u>Location</u>	<u>C₁-Amide</u>	<u>C₂-Amides</u>	<u>C₃-Amides</u>	<u>C₄-Amides</u>	<u>C₅-Amides</u>	<u>C₆-Amides</u>	<u>Ref.</u>
<u>(site type, season)</u>	<u>(pptv)</u>	<u>(pptv)</u>	<u>(pptv)</u>	<u>(pptv)</u>	<u>(pptv)</u>	<u>(pptv)</u>	

带格式表格

带格式的：缩进：首行缩进： 1 字符

带格式的：缩进：首行缩进： 1 字符

757
758
759

<u>Southampton, UK</u>							<u>Leach et al.(1999)</u>
<u>(Suburban, Spring, Summer and Autumn)</u>		<u>368-4357</u>					
<u>Shanghai, China (Urban, Summer)</u>	<u>2.3±0.7°</u>	<u>169.2±51.5°</u>	<u>778.2±899.8°</u>	<u>167.8±97.0°</u>	<u>34.5±13.3°</u>	<u>13.8±5.2°</u>	<u>This study</u>

° Mean values throughout the entire campaign ± one standard deviation.

Figure captions:

Figure 1. Influences of RH on the MS signals of methylamine (MA), trimethylamine (TMA), and propanamide (PA).

Figure 2. Influences of organics on MS signals of methylamine (MA, panels A and B), trimethylamine (TMA, panels A and B), and propanamide (PA, panels C and D). Note that the right axis is used for the signal with an identical color, and other signals correspond to the left axis.

Figure 3. High-resolution single peak fitting (custom shape) for amines and amides. During the peak deconvolution, only peaks whose areas are more than 0.5% of the total will be included in the figure legend.

Figure 4. Mass defect diagram for (A) protonated amines (C_1 - C_6) and amides (C_1 - C_6) and their clusters with ethanol, together with other species with m/z less than 163 Th in the ambient sample; and (B) all nitrogen-containing species with m/z less than 163 Th in the ambient sample. Circle diameters are proportional to $\log_{10}(\text{count rates})$.

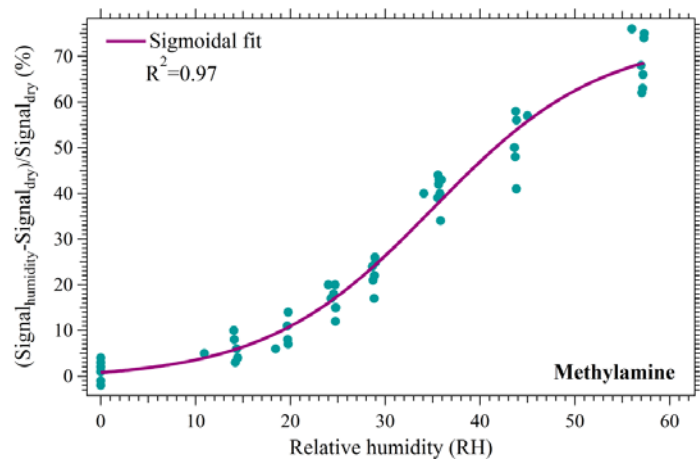
Figure 5. Time series of amines (panel A) and amides (panel B). Concentrations of amines and amides are 15-min average values.

Figure 6. Time profiles of the rainfall, C_2 -amines and C_3 -amides.

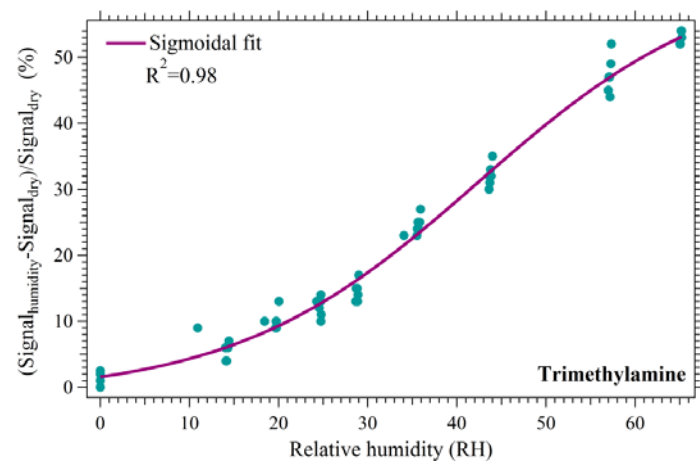
Figure 7. The averaged diurnal profiles of C_1 - and C_2 -amines and C_3 - and C_4 -amides, together with those of temperature, radiation, and ozone concentration during the campaign.

Figure 8. Three-day backward retroplumes (100 m above the ground level) from the sampling location at (A) 05:00, 12 August 2015; (B) 21:00, 20 August 2015; (C) 06:00, 21 August 2015; and (D) 06:00, 25 August 2015. The embedded boxes show 12 h backward trajectories.

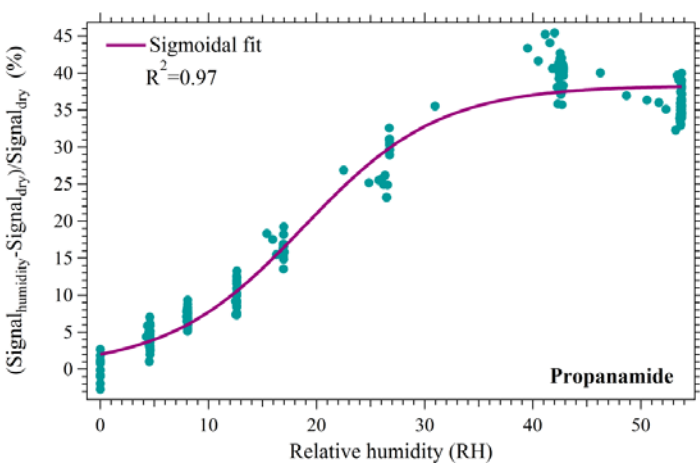
804



805



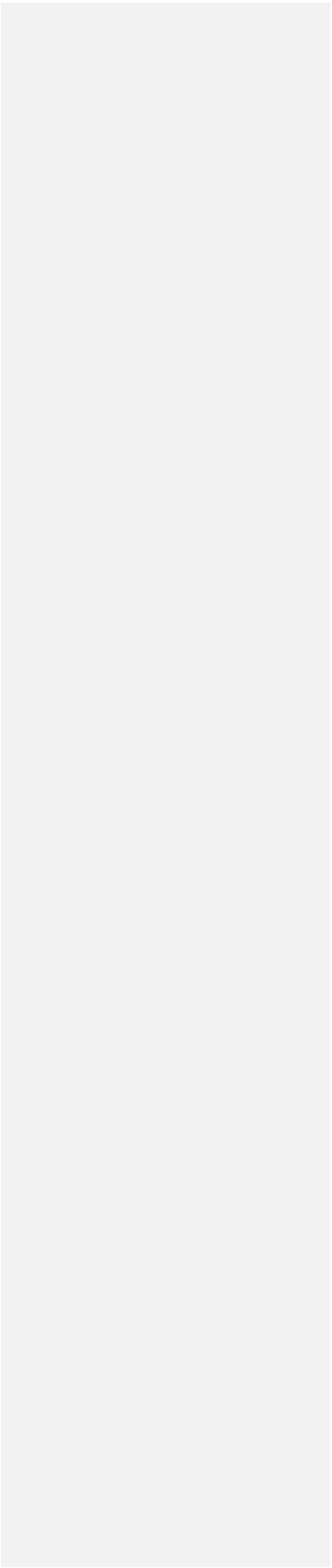
806



807

808

Figure 1



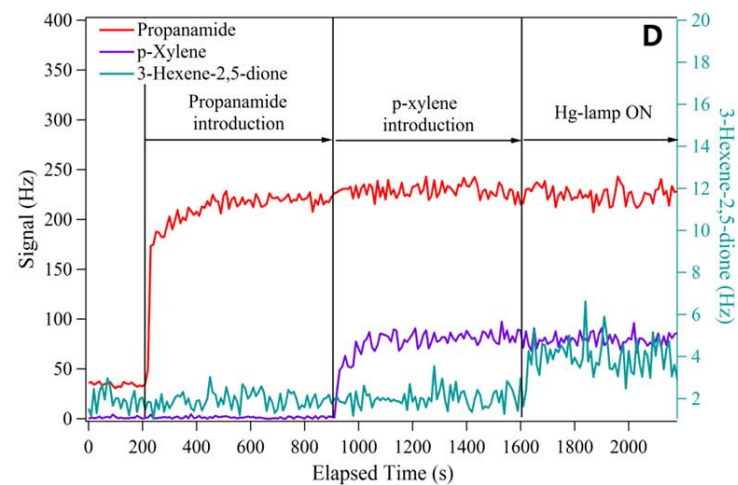
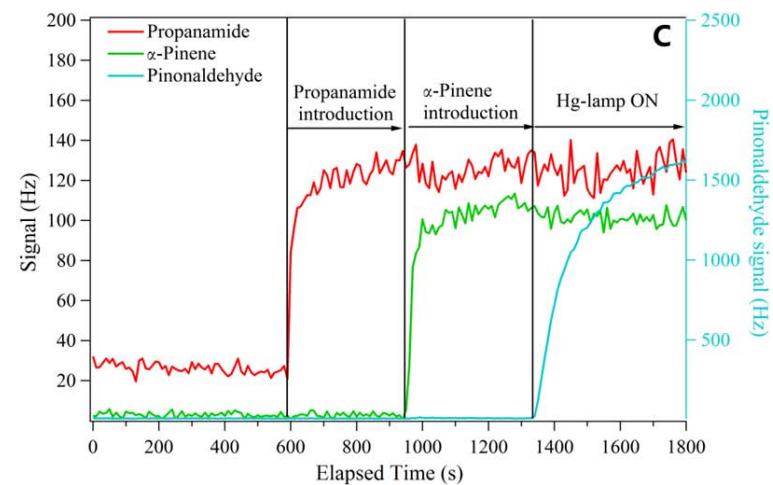
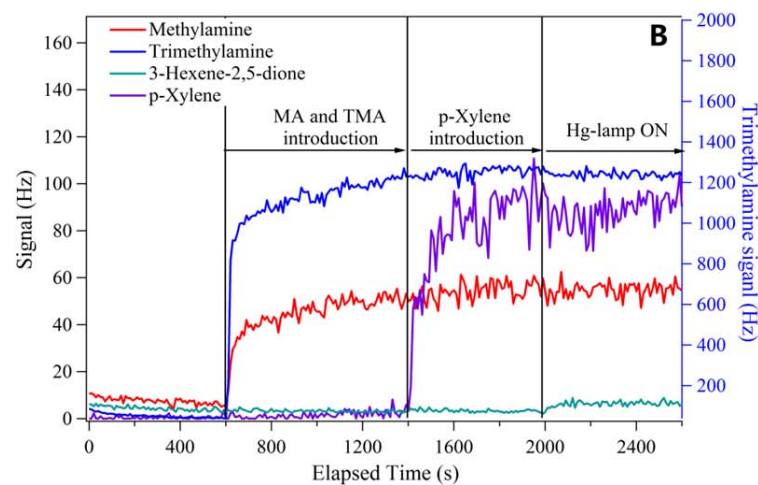
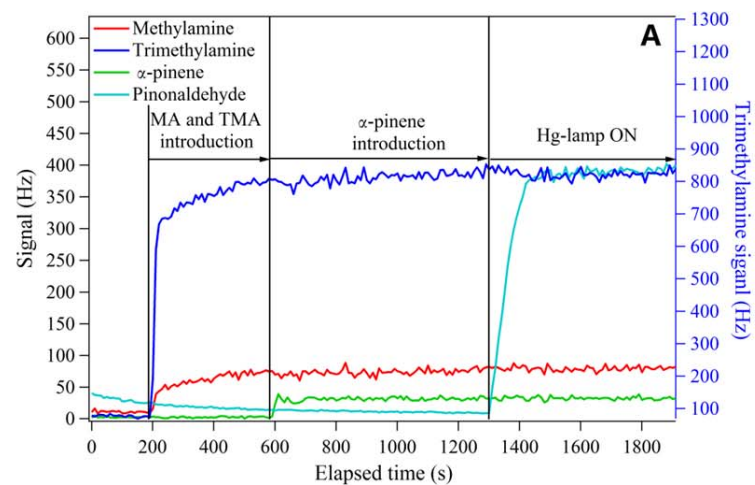
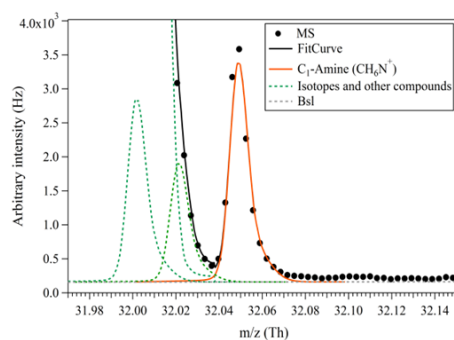
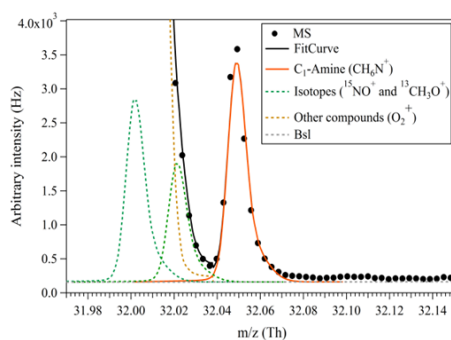
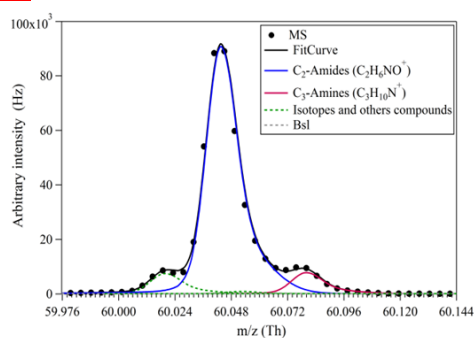
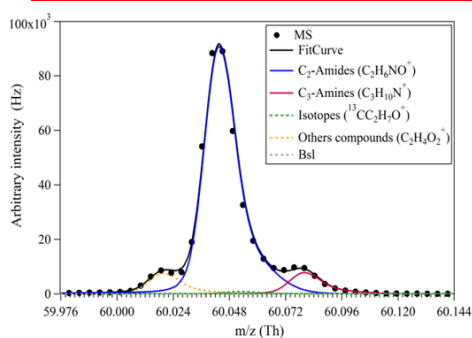
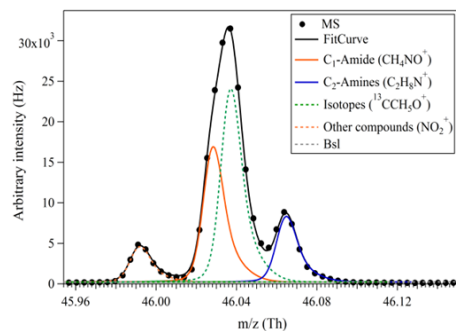
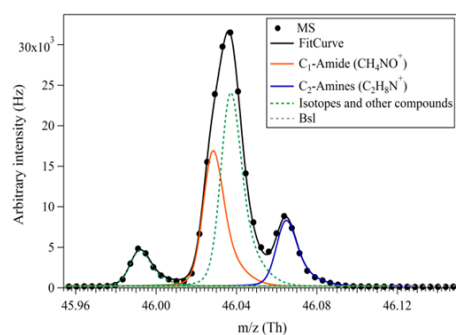


Figure 2
31

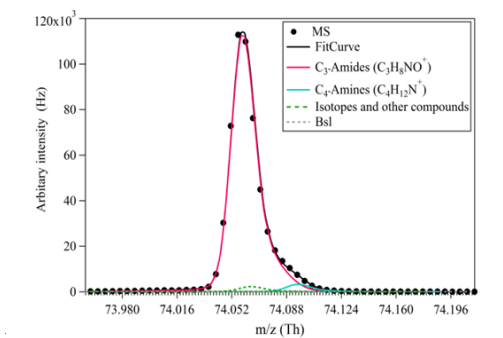


带格式的: 字体: (默认) Times
New Roman, 11 磅

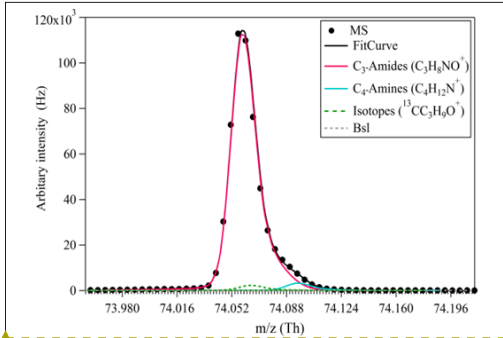


带格式的: 字体: (默认) Times
New Roman, 11 磅

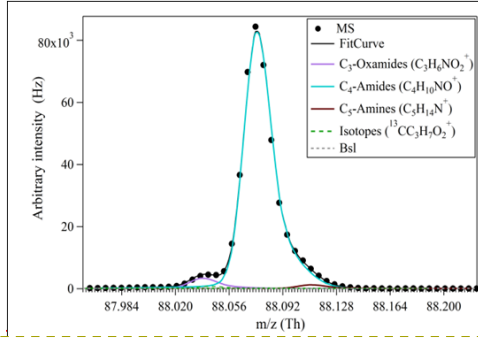
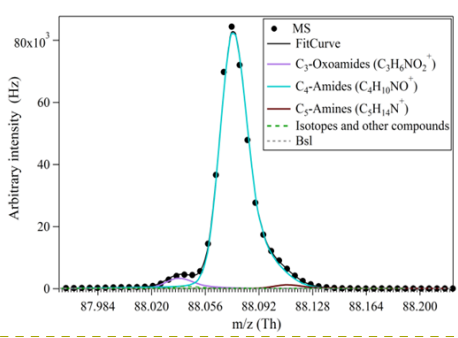
817



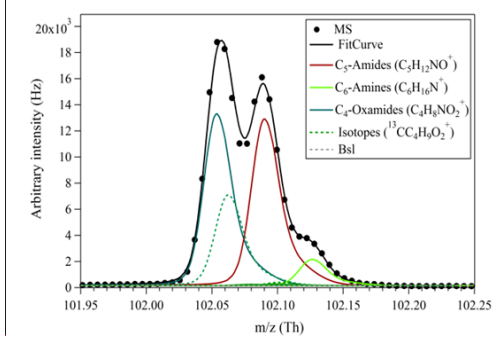
818



819



820



带格式的: 字体: (默认) Times New Roman, (中文) Times New Roman, 0 磅, 字体颜色: 黑色, 字符缩放: 0%, 边框: (无框线), 图案: 清除 (黑色)

带格式的: 字体: (默认) Times New Roman, 11 磅

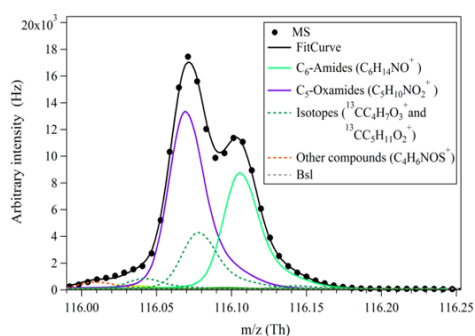
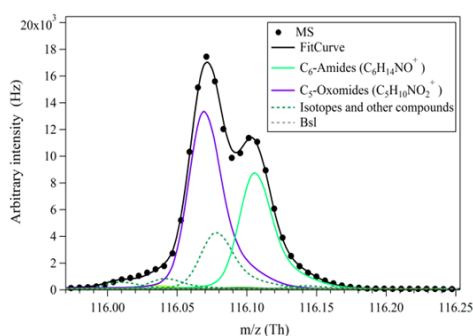
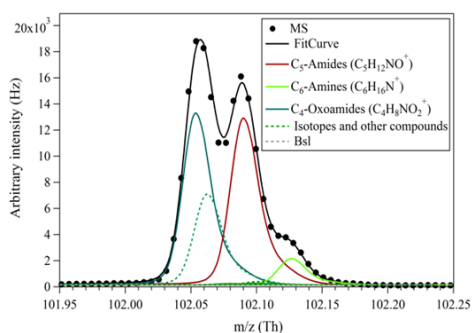
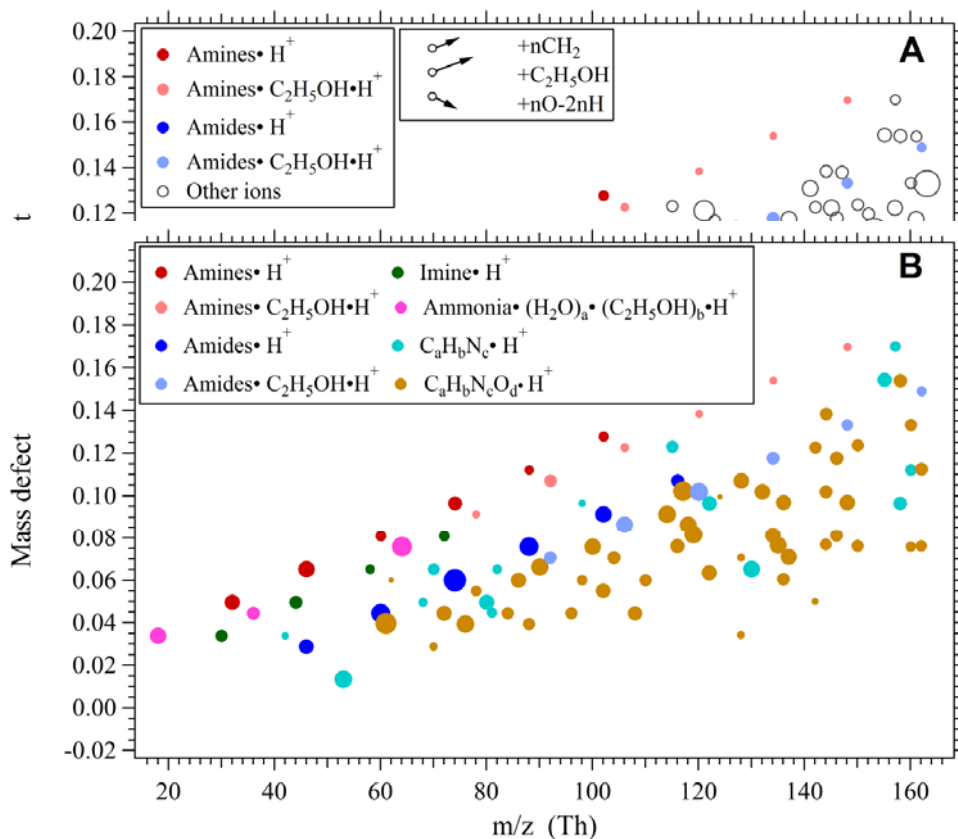
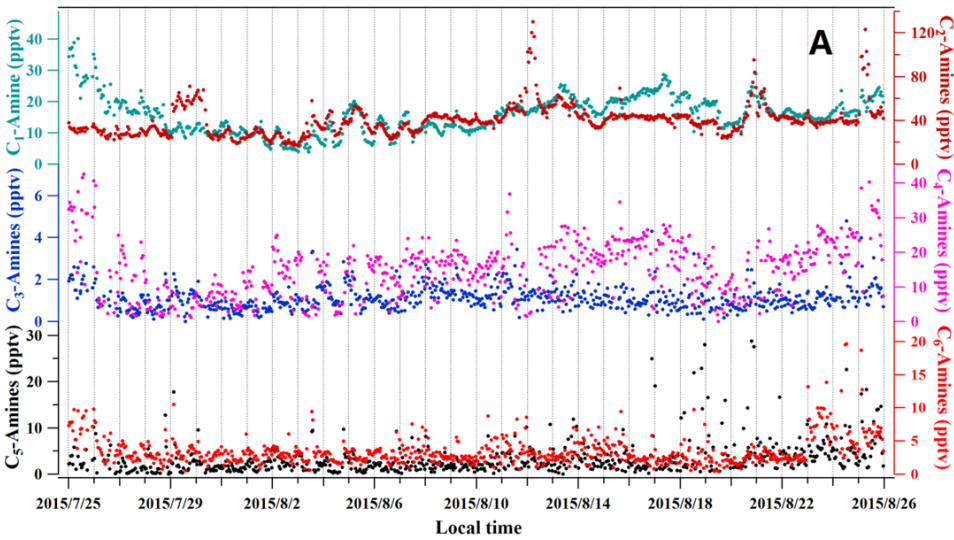


Figure 3

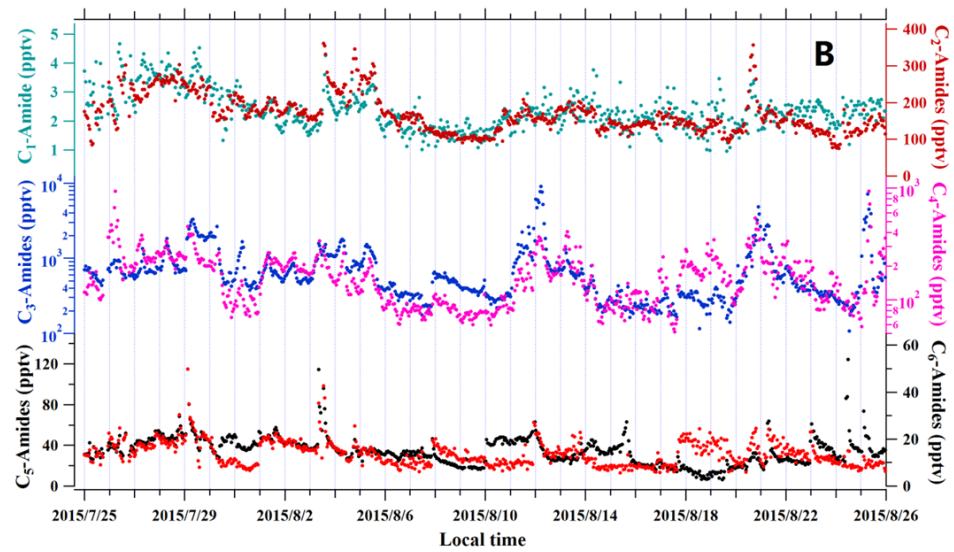


828
829
830

Figure 4



831



832
833
834
835
836
837
838
839
840
841

Figure 5

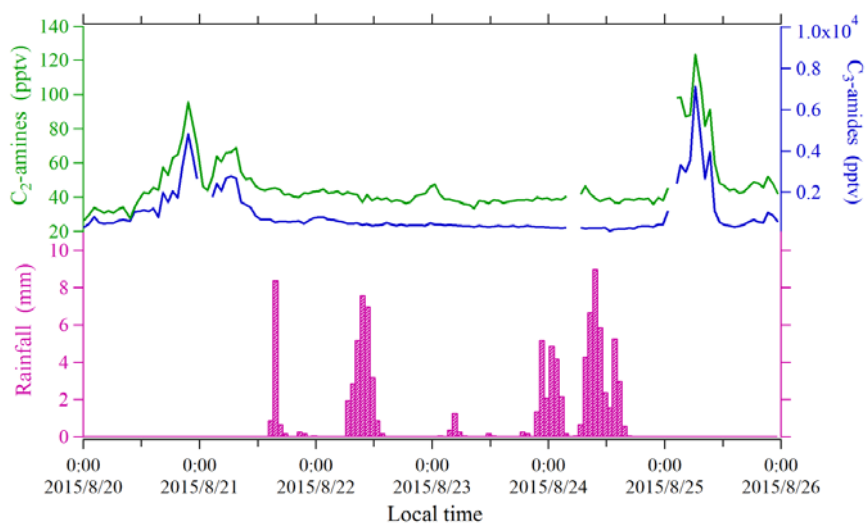


Figure 6

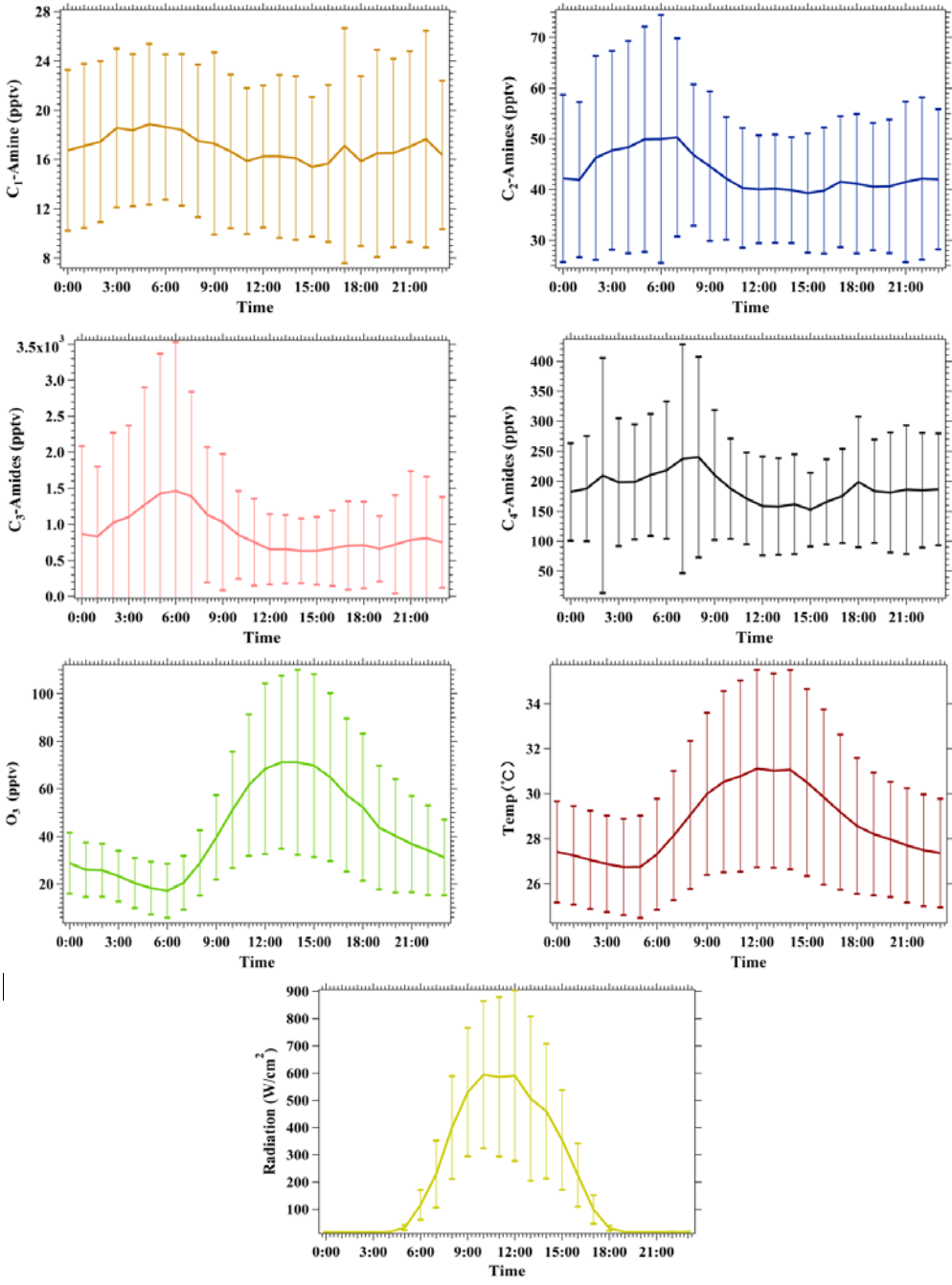


Figure 7

887

888

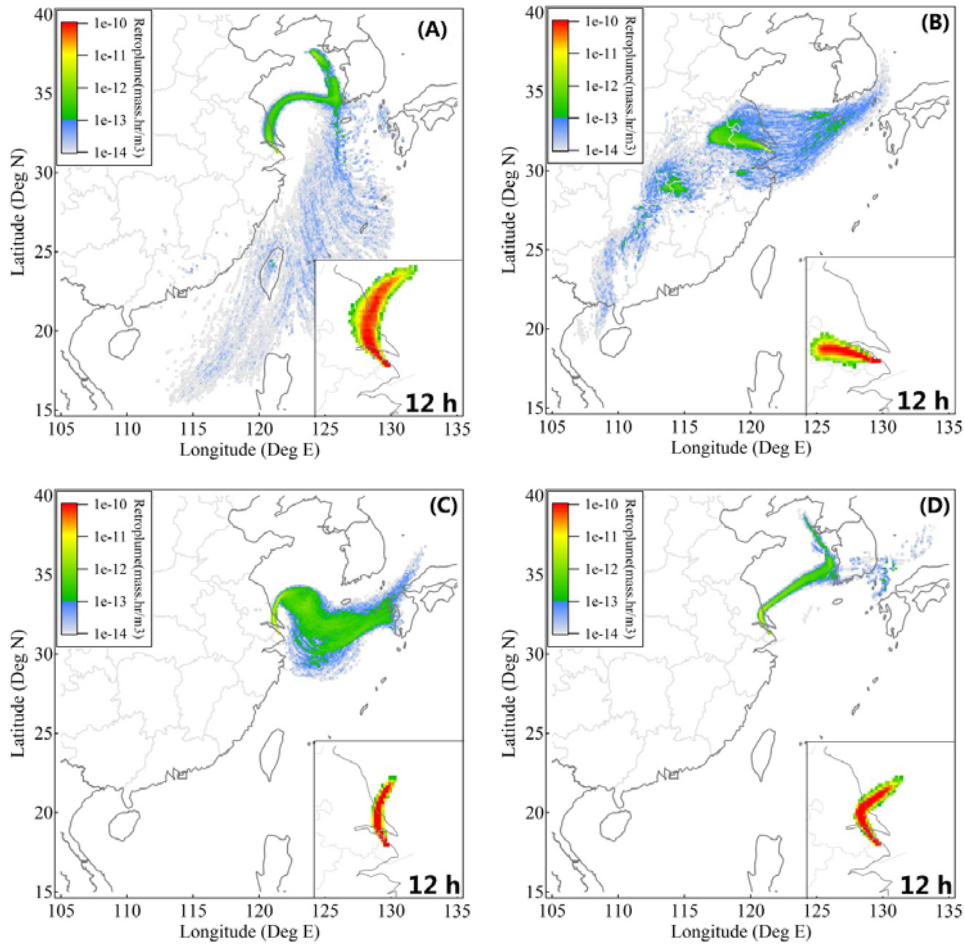


Figure 8

Supplementary Materials:

Detection of atmospheric gaseous amines and amides by a high resolution time-of-flight chemical ionization mass spectrometer with protonated ethanol reagent ions

Lei Yao¹, Ming-Yi Wang^{1,2}, Xin-Ke Wang¹, Yi-Jun Liu^{1,2,3}, Hang-Fei Chen¹, Jun Zheng^{3,4}, Wei Nie^{4,5,6}, Ai-Jun Ding^{4,5,6}, Fu-Hai Geng^{6,7}, Dong-Fang Wang^{7,8}, Jian-Min Chen¹, Douglas R. Worsnop^{8,9}, Lin Wang^{1,5,6*}

¹ Shanghai Key Laboratory of Atmospheric Particle Pollution and Prevention (LAP³), Department of Environmental Science & Engineering, Fudan University, Shanghai 200433, China

² now at Center for Atmospheric Particle Studies, Carnegie Mellon University, Pittsburgh, PA 15213, USA

²⁻³ now at Pratt School of Engineering, Duke University, Durham, NC 27705, USA

³⁻⁴ Jiangsu Key Laboratory of Atmospheric Environment Monitoring and Pollution Control, Nanjing University of Information Science & Technology, Nanjing 210044, China

⁴⁻⁵ Joint International Research Laboratory of Atmospheric and Earth System Sciences, School of Atmospheric Science, Nanjing University, 210023, Nanjing, China

⁵⁻⁶ Collaborative Innovation Center of Climate Change, Nanjing, Jiangsu Province, China

⁶⁻⁷ Shanghai Meteorology Bureau, Shanghai 200135, China

⁷⁻⁸ Shanghai Environmental Monitoring Center, Shanghai 200030, China

⁸⁻⁹ Aerodyne Research, Billerica, MA 01821, USA

* Corresponding Authors: L.W., email, lin_wang@fudan.edu.cn; phone, +86-21-65643568; fax, +86-21-65642080.

Table S1 Tentative formula assignment of MS peaks with m/z values less than 163 Th.

ID	Ion formula	Molecular weight	Potential identity
1	$\text{NH}_3 \cdot \text{H}^+$	18.0338	
2	$\text{H}_2\text{O} \cdot \text{H}^+$	19.0178	
3	$\text{HCN} \cdot \text{H}^+$	28.0182	Hydrogen cyanide
4	$\text{C}_2\text{H}_4 \cdot \text{H}^+$	29.0386	
5	$\text{CH}_3\text{N} \cdot \text{H}^+$	30.0338	
6	$\text{CH}_2\text{O} \cdot \text{H}^+$	31.0178	
7	O_2^+	31.9893	
8	$\text{CH}_5\text{N} \cdot \text{H}^+$	32.0495	Methylamine
9	$\text{CH}_4\text{O} \cdot \text{H}^+$	33.0335	
10	$\text{NH}_3 \cdot \text{H}_2\text{O} \cdot \text{H}^+$	36.0444	
11	$(\text{H}_2\text{O})_2 \cdot \text{H}^+$	37.0284	
12	$\text{C}_2\text{H}_3\text{N} \cdot \text{H}^+$	42.0338	Acetonitrile
13	$\text{C}_2\text{H}_2\text{O} \cdot \text{H}^+$	43.0178	
14	$\text{C}_2\text{H}_5\text{N} \cdot \text{H}^+$	44.0495	
15	$\text{C}_2\text{H}_4\text{O} \cdot \text{H}^+$	45.0335	
16	NO_2^+	45.9924	
17	$\text{CH}_3\text{NO} \cdot \text{H}^+$	46.0287	Formamide
18	$\text{C}_2\text{H}_7\text{N} \cdot \text{H}^+$	46.0651	C_2 -Amine
19	$\text{C}_2\text{N}_2 \cdot \text{H}^+$	53.0134	Cyanogen
20	$(\text{H}_2\text{O})_3 \cdot \text{H}^+$	55.0389	
21	$\text{C}_3\text{H}_4\text{O} \cdot \text{H}^+$	57.0335	
22	$\text{C}_4\text{H}_8 \cdot \text{H}^+$	57.0699	
23	$\text{C}_3\text{H}_7\text{N} \cdot \text{H}^+$	58.0651	
24	$\text{C}_3\text{H}_6\text{O} \cdot \text{H}^+$	59.0491	
25	$\text{C}_2\text{H}_3\text{O}_2 \cdot \text{H}^+$	60.0206	
26 25	$\text{C}_2\text{H}_5\text{NO} \cdot \text{H}^+$	60.0444	C_2 -Amide
27 26	$\text{C}_3\text{H}_9\text{N} \cdot \text{H}^+$	60.0808	C_3 -Amine
28 27	$\text{CH}_4\text{N}_2\text{O} \cdot \text{H}^+$	61.0396	
29 28	$\text{C}_2\text{H}_7\text{NO} \cdot \text{H}^+$	62.0600	2-Aminoethanol
30 29	$\text{C}_2\text{H}_6\text{O}_2 \cdot \text{H}^+$	63.0441	
31 30	$(\text{C}_2\text{H}_5\text{OH}) \cdot \text{NH}_3 \cdot \text{H}^+$	64.0757	
32 31	$(\text{C}_2\text{H}_5\text{OH}) \cdot \text{H}_2\text{O} \cdot \text{H}^+$	65.0597	
33 32	$\text{C}_4\text{H}_5\text{N} \cdot \text{H}^+$	68.0495	Pyrrole
34 33	$\text{C}_4\text{H}_4\text{O} \cdot \text{H}^+$	69.0335	
35 34	$\text{C}_5\text{H}_8 \cdot \text{H}^+$	69.0699	
36 35	$\text{C}_3\text{H}_3\text{NO} \cdot \text{H}^+$	70.0287	
37 36	$\text{C}_4\text{H}_7\text{N} \cdot \text{H}^+$	70.0651	3-Pyrroline
38 37	$\text{C}_3\text{H}_2\text{O}_2 \cdot \text{H}^+$	71.0128	
39 38	$\text{C}_4\text{H}_6\text{O} \cdot \text{H}^+$	71.0491	
40 39	$\text{C}_3\text{H}_5\text{NO} \cdot \text{H}^+$	72.0444	
41 40	$\text{C}_4\text{H}_9\text{N} \cdot \text{H}^+$	72.0808	Pyrrolidine
42 41	$\text{C}_3\text{H}_4\text{O}_2 \cdot \text{H}^+$	73.0284	

带格式的：下标

43 42	$C_4H_8O \cdot H^+$	73.0648	
44 43	$C_3H_7NO \cdot H^+$	74.0600	C ₃ -Amide
45 44	$C_4H_{11}N \cdot H^+$	74.0964	C ₄ -Amine
46 45	$C_4H_{10}O \cdot H^+$	75.0804	
47 46	$C_2H_5NO_2 \cdot H^+$	76.0393	Glycine
48 47	$C_3H_8O_2 \cdot H^+$	77.0597	
49 48	$C_2H_7NO_2 \cdot H^+$	78.0549	
50 49	$CH_3NH_2 \cdot (C_2H_5OH) \cdot H^+$	78.0913	
51 50	$C_2H_6OS \cdot H^+$	79.0212	
52 51	$C_6H_6 \cdot H^+$	79.0542	
53 52	$C_3H_8O \cdot H_2O \cdot H^+$	79.0753	
54 53	$C_5H_5N \cdot H^+$	80.0495	Pyridine
55 54	$C_4H_4N_2 \cdot H^+$	81.0447	Pyrimidine
56 55	$C_2H_6O_2 \cdot H_2O \cdot H^+$	81.0546	
57 56	$C_6H_8 \cdot H^+$	81.0699	
58 57	$C_5H_7N \cdot H^+$	82.0651	N-Methylpyrrole
59 58	$C_2H_6O \cdot (H_2O)_2 \cdot H^+$	83.0703	
60 59	$C_4H_5NO \cdot H^+$	84.0444	
61 60	$C_4H_4O_2 \cdot H^+$	85.0284	
62 61	$C_5H_8O \cdot H^+$	85.0648	
63 62	$C_4H_7NO \cdot H^+$	86.0600	
64 63	$C_4H_6O_2 \cdot H^+$	87.0441	
65 64	$C_5H_{10}O \cdot H^+$	87.0804	
66 65	$C_3H_5NO_2 \cdot H^+$	88.0393	C ₃ -Oxoamide
67 66	$C_4H_9NO \cdot H^+$	88.0757	C ₄ -Amide
68 67	$C_5H_{13}N \cdot H^+$	88.1121	C ₅ -Amine
69 68	$C_3H_4O_3 \cdot H^+$	89.0233	
70 69	$C_4H_8O_2 \cdot H^+$	89.0597	
71 70	$C_5H_{12}O \cdot H^+$	89.0961	
72 71	$C_2H_7N_3O \cdot H^+$	90.0662	
73 72	$C_4H_{10}O_2 \cdot H^+$	91.0754	
74 73	$CH_4NO \cdot (C_2H_5OH) \cdot H^+$	92.0706	
75 74	$C_2H_7N \cdot (C_2H_5OH) \cdot H^+$	92.1070	
76 75	$C_5H_5NO \cdot H^+$	96.0444	
77 76	$C_5H_4O_2 \cdot H^+$	97.0284	
78 77	$C_6H_8O \cdot H^+$	97.0648	
79 78	$C_5H_7NO \cdot H^+$	98.0600	
80 79	$C_6H_{11}N \cdot H^+$	98.0964	2,5-Dimethyl-3-pyrroline
81 80	$C_5H_6O_2 \cdot H^+$	99.0441	
82 81	$C_6H_{10}O \cdot H^+$	99.0804	
83 82	$C_5H_9NO \cdot H^+$	100.0757	
84 83	$C_5H_8O_2 \cdot H^+$	101.0597	
85 84	$C_6H_{12}O \cdot H^+$	101.0961	
86 85	$C_4H_7NO_2 \cdot H^+$	102.0550	C ₄ -Oxoamide
87 86	$C_5H_{11}NO \cdot H^+$	102.0913	C ₅ -Amide
88 87	$C_6H_{15}N \cdot H^+$	102.1277	C ₆ -Amine
89 88	$C_5H_{10}O_2 \cdot H^+$	103.0754	
90 89	$C_6H_{14}O \cdot H^+$	103.1117	

9190	$C_4H_9NO_2 \cdot H^+$	104.0706	4-Aminobutyric acid
9291	$C_5H_{12}O_2 \cdot H^+$	105.0910	
9392	$C_2H_6NO \cdot (C_2H_5OH) \cdot H^+$	106.0863	
9493	$C_3H_9N \cdot (C_2H_5OH) \cdot H^+$	106.1226	
9594	$C_6H_5NO \cdot H^+$	108.0444	
9695	$C_8H_{12} \cdot H^+$	109.1012	
9796	$C_6H_7NO \cdot H^+$	110.0600	
9897	$C_6H_6O_2 \cdot H^+$	111.0441	
9998	$C_6H_8O_2 \cdot H^+$	113.0597	
10099	$C_6H_{11}NO \cdot H^+$	114.0913	
101400	$C_5H_6O_3 \cdot H^+$	115.0390	
102401	$C_6H_{10}O_2 \cdot H^+$	115.0754	
103402	$C_6H_{14}N_2 \cdot H^+$	115.1230	2,5-Dimethylpiperazine
104	$C_4H_5NOS \cdot H^+$	116.0165	
105403	$C_5H_9NO_2 \cdot H^+$	116.0760	C ₅ -Oxoamide
106404	$C_6H_{13}NO \cdot H^+$	116.1070	C ₆ -Amide
107405	$C_5H_8O_3 \cdot H^+$	117.0546	
108406	$C_6H_{12}O_2 \cdot H^+$	117.0910	
109407	$C_5H_{12}N_2O \cdot H^+$	117.1022	
110408	$C_5H_{11}NO_2 \cdot H^+$	118.0863	L-Valine
111409	$C_4H_{10}N_2O_2 \cdot H^+$	119.0815	
112410	$C_6H_{14}O_2 \cdot H^+$	119.1067	
113411	$C_5H_{11}OS \cdot H^+$	120.0570	
114412	$C_3H_7NO \cdot (C_2H_5OH) \cdot H^+$	120.1019	
115413	$C_4H_{12}N \cdot (C_2H_5OH) \cdot H^+$	120.1383	
116414	$C_8H_8O \cdot H^+$	121.0648	
117415	$C_6H_{14}O \cdot H_2O \cdot H^+$	121.1210	
118416	$C_4H_{11}NOS \cdot H^+$	122.0634	
119417	$C_8H_{11}N \cdot H^+$	122.0964	Phenethylamine
120418	$C_4H_{10}O_2S \cdot H^+$	123.0474	
121419	$C_8H_{10}O \cdot H^+$	123.0804	
122420	$C_9H_{14} \cdot H^+$	123.1168	
123421	$C_3H_9NO_2S \cdot H^+$	124.0995	
124422	$C_7H_8O_2 \cdot H^+$	125.0597	
125423	$C_8H_{12}O \cdot H^+$	125.0961	
126424	$C_6H_6O_3 \cdot H^+$	127.0390	
127425	$C_7H_{10}O_2 \cdot H^+$	127.0753	
128426	$C_8H_{14}O \cdot H^+$	127.1117	
129427	$C_5H_5NO_3 \cdot H^+$	128.0342	
130428	$C_6H_9NO_2 \cdot H^+$	128.0706	
131429	$C_7H_{13}NO \cdot H^+$	128.1070	
132430	$C_7H_{12}O_2 \cdot H^+$	129.0910	
133431	$C_9H_7N \cdot H^+$	130.0651	Quinoline
134432	$C_6H_{10}O_3 \cdot H^+$	131.0702	
135433	$C_7H_{14}O_2 \cdot H^+$	131.1067	
136434	$C_6H_{13}NO_2 \cdot H^+$	132.1019	L-Leucine
137435	$C_6H_{12}O_3 \cdot H^+$	133.0859	
138436	$C_3H_5NO_2 \cdot (C_2H_5OH) \cdot H^+$	134.0812	

139 137	$C_4H_9NO \cdot (C_2H_5OH) \cdot H^+$	134.1176	
140 138	$C_5H_{13}N \cdot (C_2H_5OH) \cdot H^+$	134.1539	
141 139	$C_8H_6O_2 \cdot H^+$	135.0441	
142 140	$C_4H_{10}N_2O_3 \cdot H^+$	135.0764	
143 141	$C_6H_{14}O_3 \cdot H^+$	135.1016	
144 142	$C_7H_5NS \cdot H^+$	136.0215	
145 143	$C_4H_9NO_4 \cdot H^+$	136.0604	
146 144	$C_5H_{13}NO_3 \cdot H^+$	136.0968	
147 145	$C_7H_8N_2O \cdot H^+$	137.0709	
148 146	$C_9H_{12}O \cdot H^+$	137.0961	
149 147	$C_6H_{14}O_2 \cdot H_2O \cdot H^+$	137.1172	
150 148	$C_4H_{11}NO_2S \cdot H^+$	138.1039	
151 149	$C_7H_8O_3 \cdot H^+$	141.0546	
152 150	$C_8H_{12}O_2 \cdot H^+$	141.0910	
153 151	$C_9H_{16}O \cdot H^+$	141.1308	
154 152	$C_6H_7NO_3 \cdot H^+$	142.0499	
155 153	$C_8H_{15}NO \cdot H^+$	142.1226	
156 154	$C_7H_{10}O_3 \cdot H^+$	143.0703	
157 155	$C_8H_{14}O_2 \cdot H^+$	143.1067	
158 156	$C_8H_{18}N_2 \cdot H^+$	143.1542	1-Butylpiperazine
159 157	$C_5H_9N_3O_2 \cdot H^+$	144.0768	
160 158	$C_7H_{13}NO_2 \cdot H^+$	144.1019	
161 159	$C_8H_{17}NO \cdot H^+$	144.1383	
162 160	$C_6H_8O_4 \cdot H^+$	145.0495	
163 161	$C_7H_{12}O_3 \cdot H^+$	145.0859	
164 162	$C_8H_{16}O_2 \cdot H^+$	145.1223	
165 163	$C_6H_{11}NO_3 \cdot H^+$	146.0811	
166 164	$C_7H_{15}NO_2 \cdot H^+$	146.1176	7-Aminoheptanoic acid
167 165	$C_6H_{10}O_4 \cdot H^+$	147.0652	
168 166	$C_7H_{14}O_3 \cdot H^+$	147.1016	
169 167	$C_8H_{18}O_2 \cdot H^+$	147.1379	
170 168	$C_4H_7NO_2 \cdot (C_2H_5OH) \cdot H^+$	148.0968	
171 169	$C_5H_{11}NO \cdot (C_2H_5OH) \cdot H^+$	148.1332	
172 170	$C_6H_{15}N \cdot (C_2H_5OH) \cdot H^+$	148.1696	
173 171	$C_5H_8O_3S \cdot H^+$	149.0267	
174 172	$C_9H_8O_2 \cdot H^+$	149.0597	
175 173	$C_6H_{12}O_4 \cdot H^+$	149.0808	
176 174	$C_8H_7NS \cdot H^+$	150.0372	
177 175	$C_5H_{11}NO_4 \cdot H^+$	150.0761	
178 176	$C_5H_{15}N_3O_2 \cdot H^+$	150.1237	
179 177	$C_5H_{14}N_2OS \cdot H^+$	151.0899	
180 178	$C_{10}H_{14}O \cdot H^+$	151.1117	
181 179	$C_7H_5NOS \cdot H^+$	152.0165	
182 180	$C_{10}H_{15}O \cdot H^+$	152.1196	
183 181	$C_6H_{14}O_3 \cdot H_2O \cdot H^+$	153.1121	
184 182	$C_9H_{14}O_2 \cdot H^+$	155.1067	
185 183	$C_9H_{18}N_2 \cdot H^+$	155.1543	4-Pyrrolidinopiperidine
186 184	$C_8H_{12}O_3 \cdot H^+$	157.0859	

187 185	$C_9H_{16}O_2 \cdot H^+$	157.1223	
188 186	$C_9H_{20}N_2 \cdot H^+$	157.1699	Triacetonediamine
189 187	$C_{11}H_{11}N \cdot H^+$	158.0964	2,8-Dimethylquinoline
190 188	$C_9H_{19}NO \cdot H^+$	158.1539	
191 189	$C_7H_{10}O_4 \cdot H^+$	159.0652	
192 190	$C_8H_{14}O_3 \cdot H^+$	159.1016	
193 191	$C_{10}H_9NO \cdot H^+$	160.0757	
194 192	$C_{11}H_{13}N \cdot H^+$	160.1121	2,3,3-Trimethylindolenine
195 193	$C_8H_{17}NO_2 \cdot H^+$	160.1332	8-Aminooctanoic acid
196 194	$C_7H_{12}O_4 \cdot H^+$	161.0808	
197 195	$C_8H_{16}O_3 \cdot H^+$	161.1172	
198 196	$C_9H_{20}O_2 \cdot H^+$	161.1536	
199 197	$C_4H_5NO_3 \cdot (C_2H_5OH) \cdot H^+$	162.0761	
200 198	$C_5H_9NO_2 \cdot (C_2H_5OH) \cdot H^+$	162.1125	
201 199	$C_6H_{13}NO \cdot (C_2H_5OH) \cdot H^+$	162.1489	
202 200	$C_8H_{18}O_3 \cdot H^+$	163.1329	

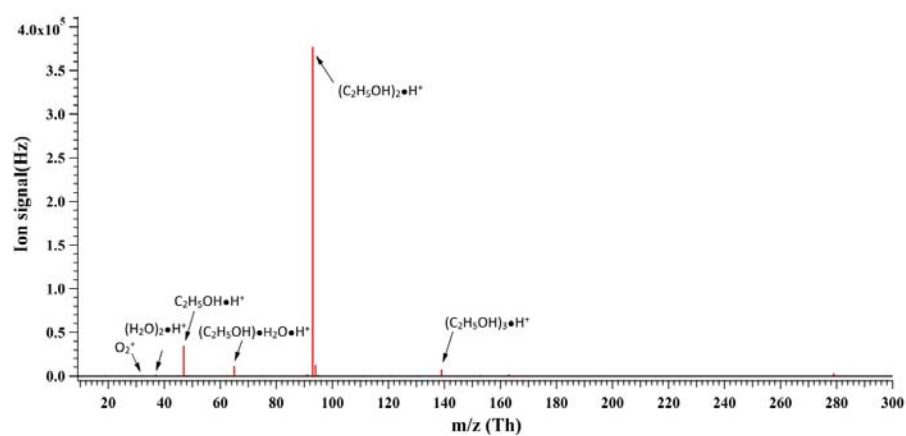


Figure S1. A typical mass spectrum with $RH < 20\%$. The dominant reagent ions are protonated ethanol dimer ($(C_2H_5OH)_2 \cdot H^+$), monomer ($(C_2H_5OH) \cdot H^+$), and trimer ($(C_2H_5OH)_3 \cdot H^+$). The ratio of the clusters of protonated ethanol with water ($C_2H_5OH \cdot H_2O \cdot H^+$) to the sum of $(C_2H_5OH) \cdot H^+$, $(C_2H_5OH)_2 \cdot H^+$, and $(C_2H_5OH)_3 \cdot H^+$ is ~ 0.026 .

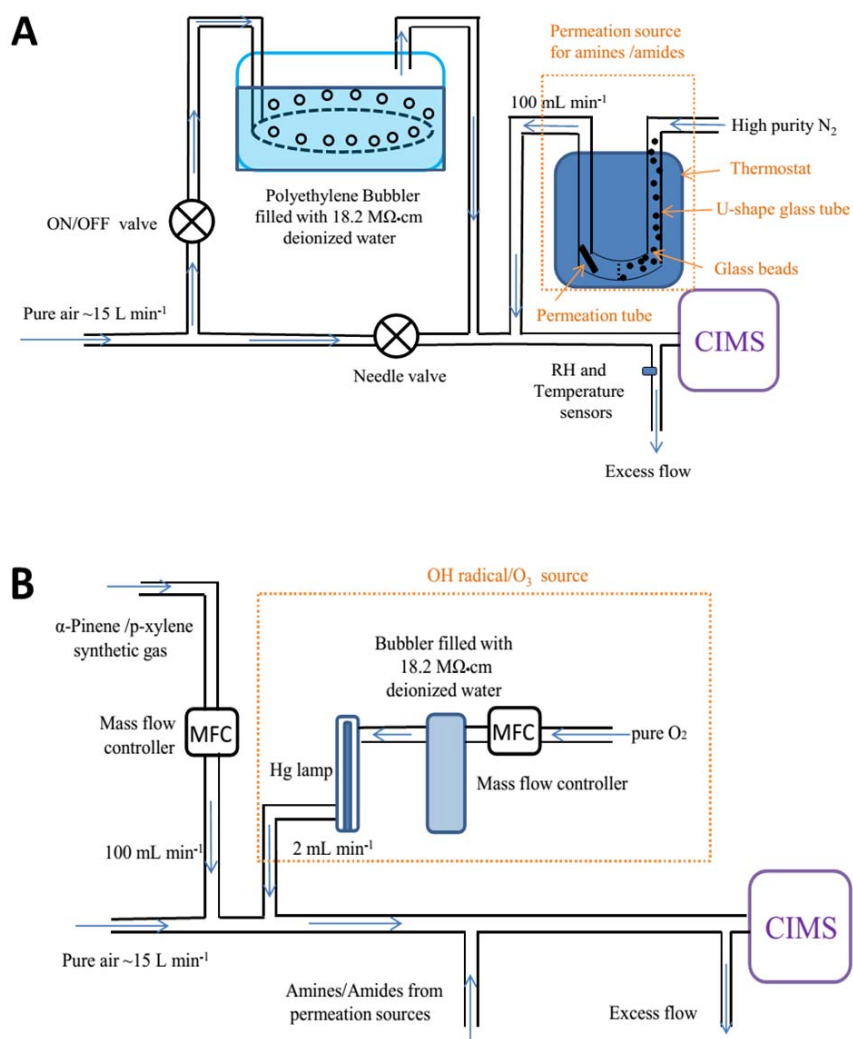


Figure S2. Schematics for laboratory tests of effects of (A) RH and (B) organics. All sampling lines are made of PFA or PTFE material.

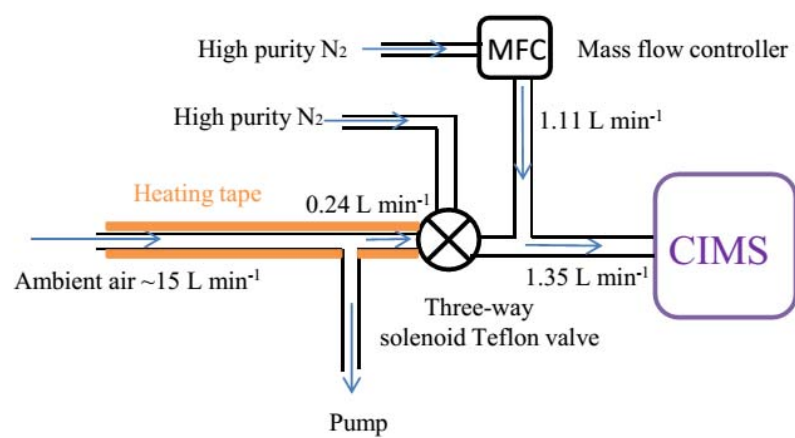


Figure S3. Schematic of CIMS setup during the field measurements.

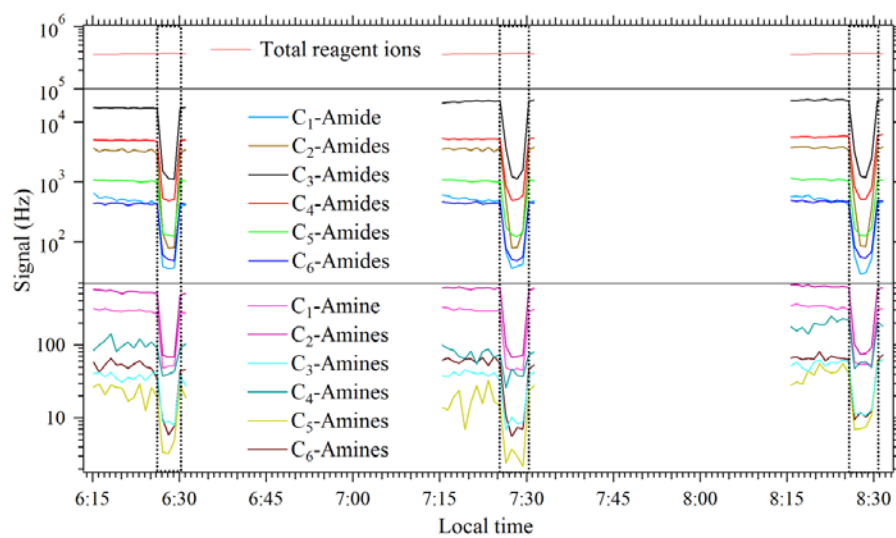


Figure S4. Background check for amines and amides during a 3 h ambient sampling period.

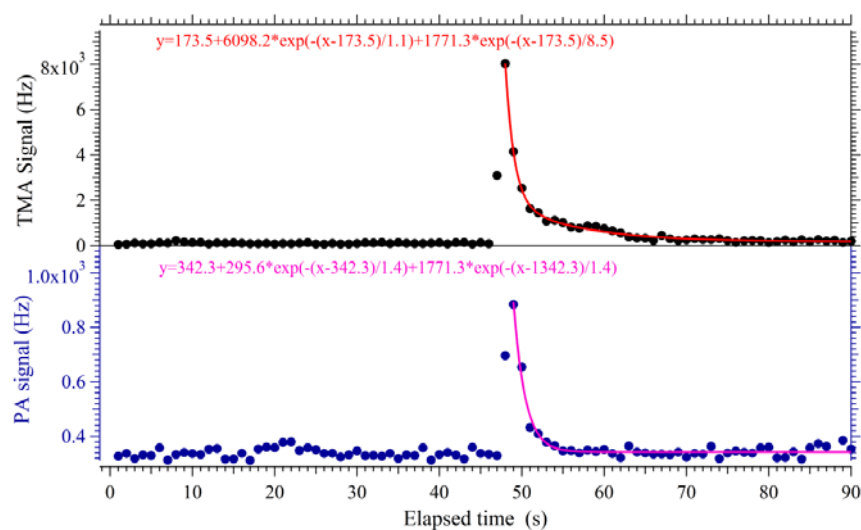


Figure S5. Inlet memory of TMA and PA by inlet spike tests. The red and pink curves are fittings by the sum of two decaying exponentials. The characteristic decaying times of two exponentials, which are displacement of amines and amides inside the inlet by pumping and removing amines and amides adsorbed on the inlet surface, were 1.1 s and 8.5 s for TMA, and 1.4 s and 1.4 s for PA, respectively.

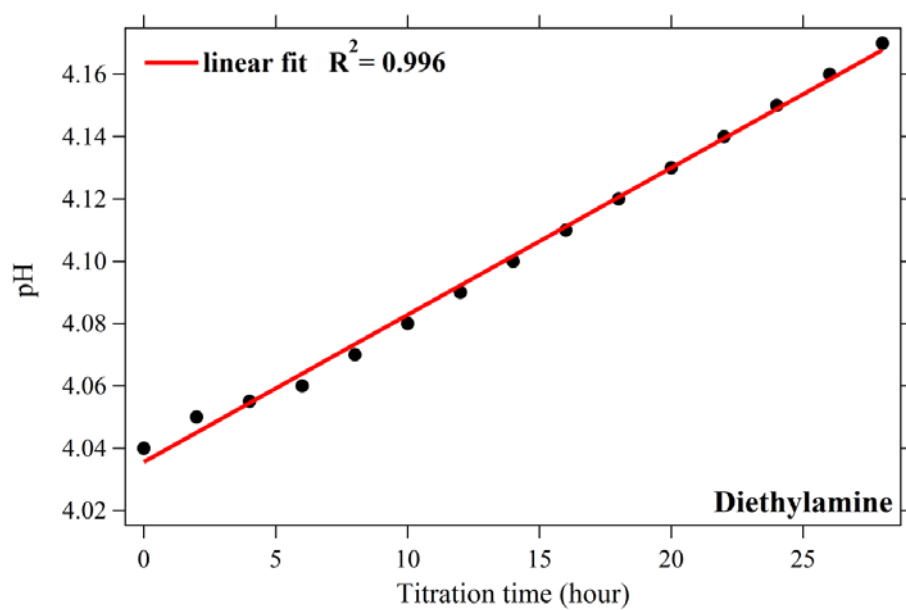


Figure S6. Changes in pH values of HNO₃ solution as titration by diethylamine proceeds. Note that pH values in this plot are 2-h averages

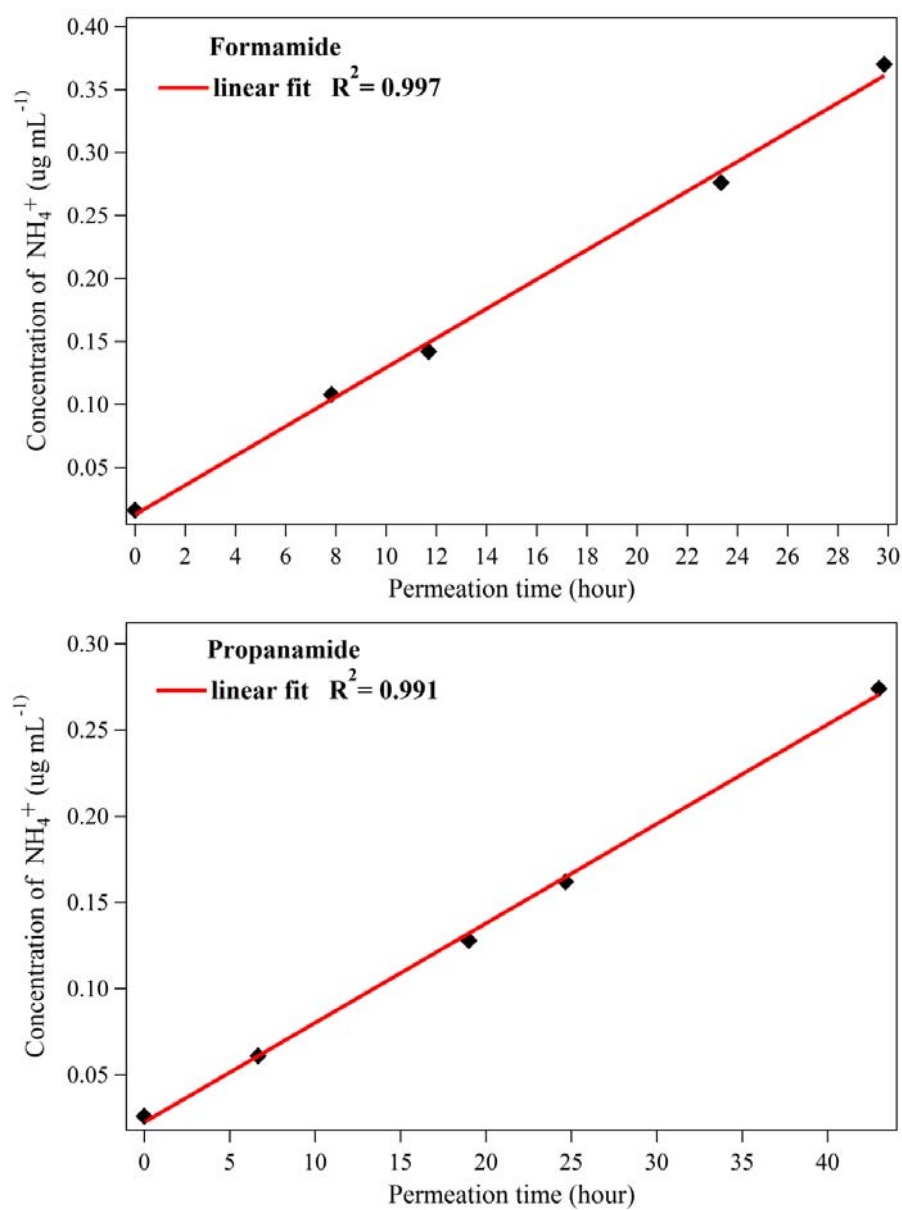


Figure S7. Changes in NH_4^+ concentration as hydrolysis of formamide and propanamide proceeds.

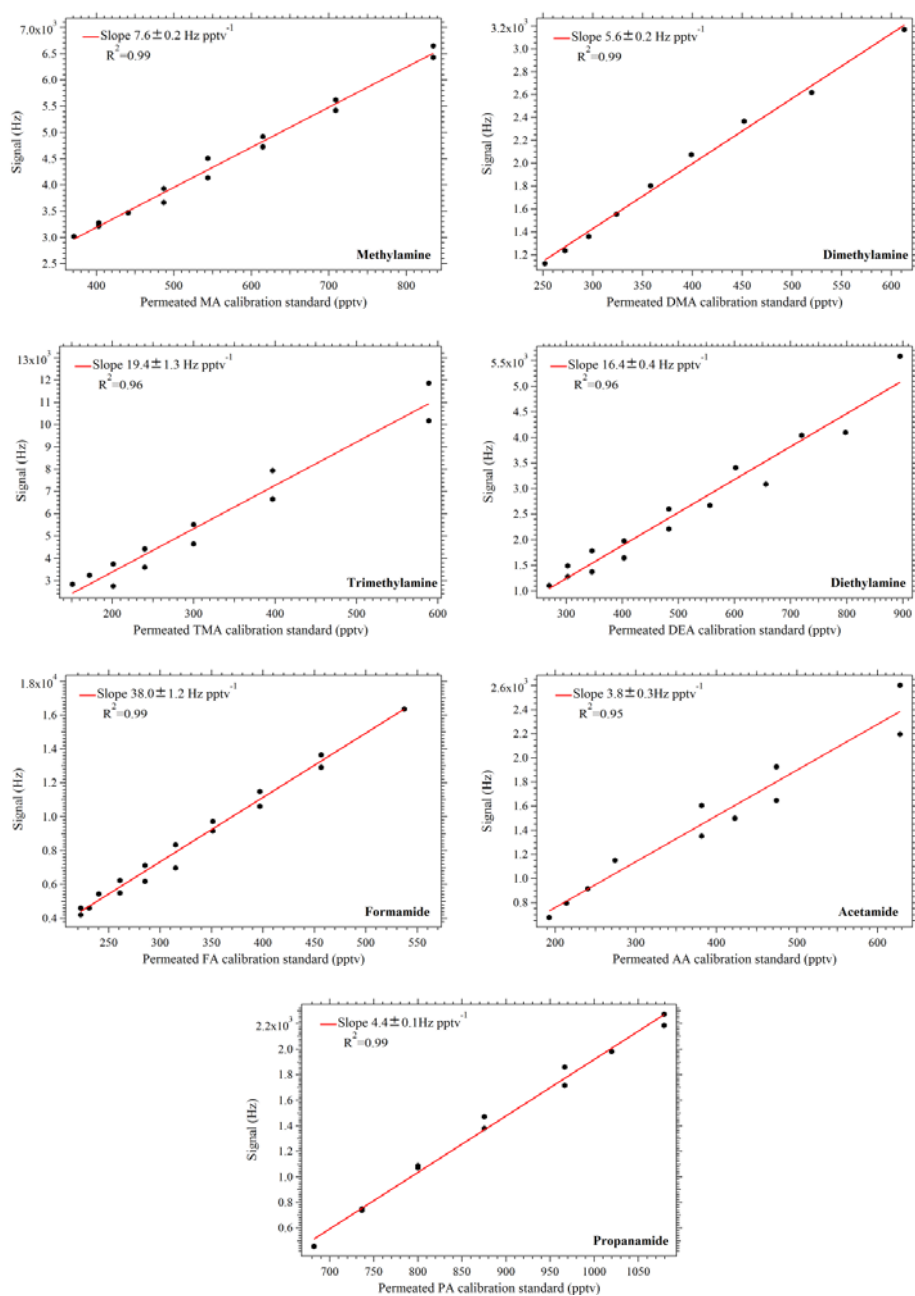


Figure S8. Calibration curves of C₁- to C₄-amines (MA, DMA, TMA, and DEA) and C₁- to C₃-amides (FA, AA, and PA). The red solid lines are linear fittings to guide the eye and the slopes are sensitivities for detection.

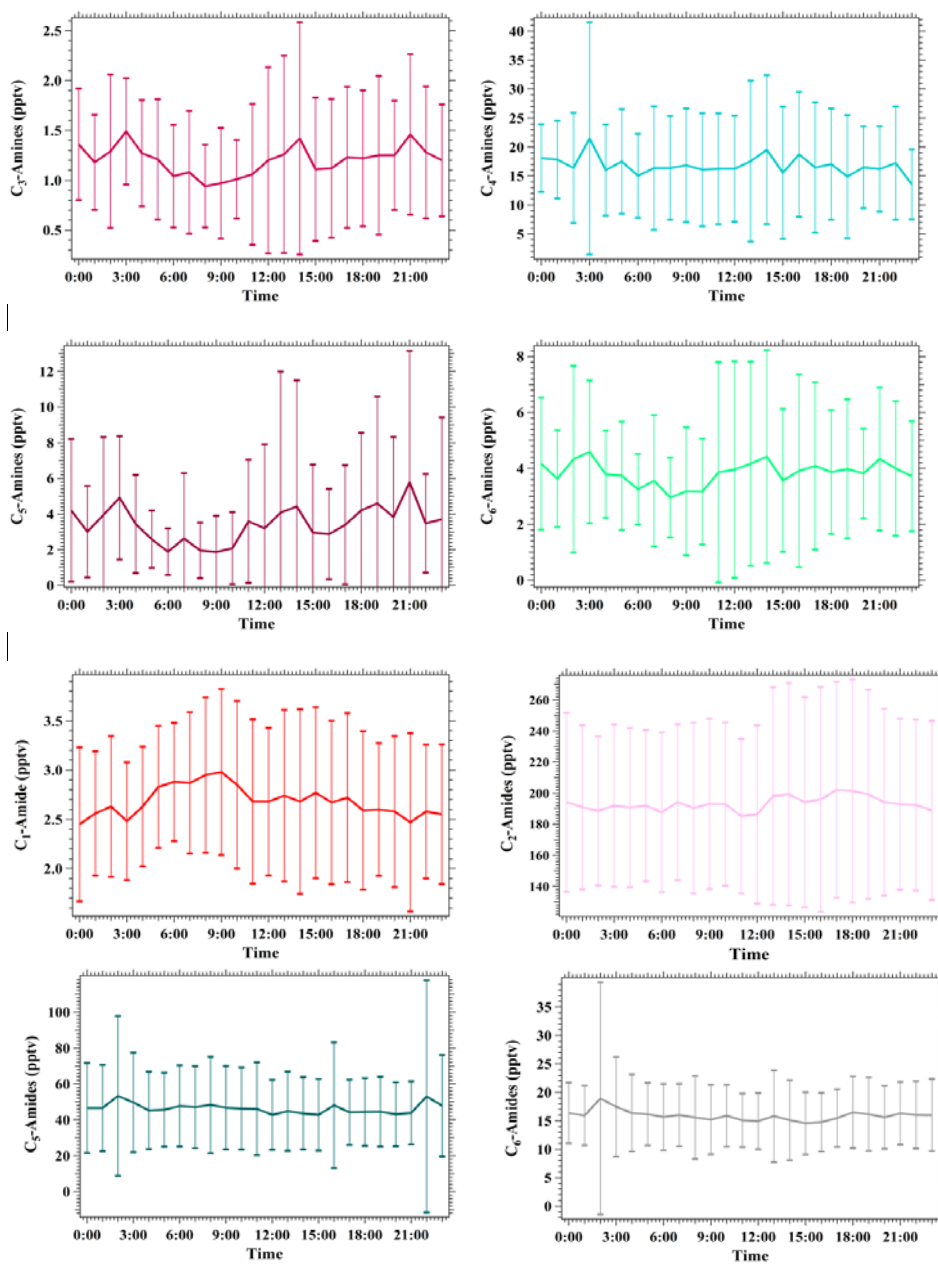


Figure S9. Diurnal variations of amines and amides with less variation^{SS}.

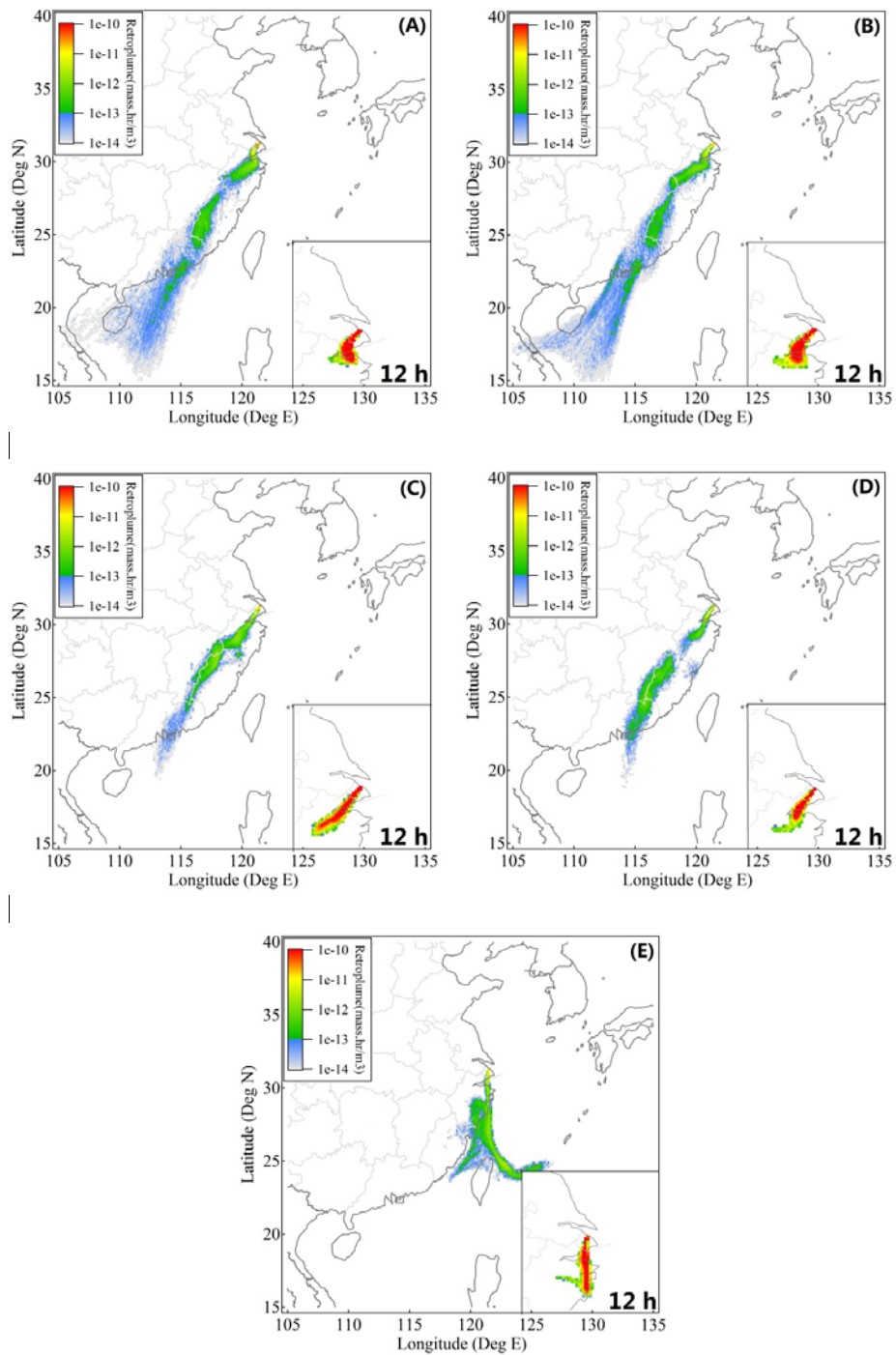


Figure S10. Three-day backward retroplumes (100 m above the ground level) from the sampling location at **(A)** 07:00, 27 July 2015; **(B)** 07:00, 28 July 2015; **(C)** 07:00, 30 July 2015; **(D)** 07:00, 31 July 2015; and **(E)** 07:00, 4 August 2015. The embedded boxes show 12h backward trajectories.